Phospholipase D activity couples plasma membrane endocytosis with retromer dependent recycling.

Rajan Thakur[%]*, Aniruddha Panda[^]*, Elise Coessens[@], Nikita Raj*, Shweta Yadav*, Sruthi Balakrishnan*, Qifeng Zhang[@], Plamen Georgiev[@], Bishal Basak*, Renu Pasricha*, Michael J.O. Wakelam[@], Nicholas Ktistakis[@] and Padinjat Raghu*

*National Centre for Biological Sciences, TIFR-GKVK Campus, Bellary Road, Bangalore 560065,India

[@]Inositide Laboratory, Babraham Institute, Cambridge CB22 3AT, United Kingdom

[^]Manipal University, Madhav Nagar, Manipal 576104, Karnataka, India

[%]Shanmugha Arts, Science, Technology & Research Academy, Thanjavur 613401, India

Abstract

During illumination, the light sensitive plasma membrane (rhabdomere) of *Drosophila* photoreceptors undergoes turnover with consequent changes in size and composition. However the mechanism by which illumination is coupled to rhabdomere turnover remains unclear. We find that photoreceptors contain a light-dependent phospholipase D (PLD) activity. During illumination, loss of PLD resulted in an enhanced reduction in rhabdomere size, accumulation of Rab7 positive, rhodopsin1-containing vesicles (RLVs) in the cell body and reduced rhodopsin protein. These phenotypes were associated with reduced levels of phosphatidic acid, the product of PLD activity and were rescued by reconstitution with catalytically active PLD. In wild type photoreceptors, during illumination, enhanced PLD activity was sufficient to clear RLVs from the cell body by a process dependent on Arf1-GTP levels and retromer complex function. Thus, during illumination, PLD activity couples endocytosis of RLVs with their recycling to the plasma membrane thus maintaining plasma membrane size and composition.

Introduction

The ability to detect photons is a fundamental property of animal photoreceptors. In order to achieve this, ocular photoreceptors of animals generate an expanded region of plasma membrane that is packed with the receptor for light, rhodopsin. This strategy is used regardless of the architecture of the photoreceptor. For example, in ciliary photoreceptors (e.g vertebrate rods), light passes along the outer segment that is stacked with membranous discs while in insect photoreceptors, the plasma membrane is expanded to form actin based microvilli; both of these structures are packed with rhodopsin and incident light is absorbed as it passes along them (Arendt, 2003). The light-sensitive membranes of photoreceptors undergo stimulus dependent turnover (LaVail, 1976; White and Lord, 1975); such turnover will alter both membrane area and composition, thus regulating sensitivity to light [reviewed in (Blest, 1988)]. The importance of this process is underscored by the human disease Best's macular dystrophy, in which rod outer segment length and electroretinograms are altered during changes in ambient illumination, ultimately leading to macular degeneration (Abràmoff et al., 2013). Despite the importance of this process, the cellular and molecular mechanisms that regulate photosensitive membrane turnover remains poorly understood.

In *Drosophila* photoreceptors, the apical domain is expanded to form ca. 40000 projections of light-sensitive plasma membrane (microvilli) that form the rhabdomere. Photons that are absorbed trigger G-protein coupled phospholipase C (PLC) activity that culminates in the activation of the plasma membrane channels TRP and TRPL; the resulting Ca^{2+} influx triggers an electrical response to light (Hardie and Raghu, 2001). Additionally photon absorption by rhodopsin1 (Rh1) also triggers the rhodopsin cycle [reviewed in (Raghu et al., 2012)]. Following photon absorption, Rh1 undergoes photoisomerization to meta-rhodopsin (M). M is

61 phosphorylated at its C-terminus, binds β-arrestin and this complex is removed from the
62 microvillar membrane via clathrin-dependent endocytosis to be either recycled back to the
63 microvillar plasma membrane (Wang et al., 2014) or trafficked to the lysosomes for
64 degradation (Chinchore et al., 2009)[reviewed in (Xiong and Bellen, 2013)]. Tight regulation of
65 this process is critical for rhabdomere integrity during illumination as mutants defective in any
66 of the several steps of the rhodopsin cycle undergo light-dependent collapse of the
67 rhabdomere [reviewed in (Raghu et al., 2012)]. However the process that couples endocytosis
68 of rhabdomere membrane to plasma membrane recycling remains poorly understood.

69 Phospholipase D (PLD) is an enzyme that hydrolyzes phosphatidylcholine (PC) to generate
70 phosphatidic acid (PA). In yeast, loss of PLD (*spo14*) results in a sporulation defect, failure to
71 synthesize PA (Rudge et al., 2001) and accumulation of undocked membrane vesicles on the
72 spindle pole body (Nakanishi et al., 2006). The v-SNARE Spo20p binds PA *in vitro* (De Los
73 Santos and Neiman, 2004) and is required to dock Spo20p to target membranes; in this setting
74 PA generated by PLD appears to regulate a vesicular transport process. The potential role of
75 PA in controlling vesicular transport also arose from observations *in vitro* that Arf proteins, key
76 regulators of vesicular transport, stimulate mammalian PLD activity (Brown et al., 1993;
77 Cockcroft et al., 1994). Overexpression of PLD1 in a range of neuronal (Cai et al., 2006; Vitale
78 et al., 2001) and non-neuronal cells (Choi et al., 2002; Cockcroft et al., 2002; Huang et al.,
79 2005) suggests that PLD can regulate vesicular transport. A previous study showed that
80 elevated PA levels during development of *Drosophila* photoreceptors disrupts rhabdomere
81 biogenesis with associated endomembrane defects (Raghu et al., 2009) that were Arf1-
82 dependent. However, the mechanism underlying the role of PLD in regulating membrane
83 transport has remained unclear and to date, no study in metazoans has demonstrated a role, if

any, for endogenous PLD in regulating vesicular transport *in vivo*. In this study, we show that during illumination in *Drosophila* photoreceptors, rhabdomere size is regulated through the turnover of apical plasma membrane via RLVs. We find that photoreceptors have a light-regulated PLD activity that is required to maintain PA levels during illumination and support apical membrane size. PLD works in coordination with retromer function and Arf1 activity to regulate apical membrane size during illumination. Thus PLD is a key regulator of plasma membrane turnover during receptor activation and signaling in photoreceptors.

Results

Rhabdomere size and Rh1 levels are modulated by illumination in *Drosophila*

We quantified rhabdomere size of *Drosophila* photoreceptors during illumination by transmission electron microscopy (TEM) followed by volume fraction analysis. When wild type flies are grown in white light for 48 hours (hrs) post-eclosion, the volume fraction (V_f) of the cell occupied by the rhabdomere in photoreceptors R1-R6 was reduced (Fig 1A,B). This reduction in V_f occurred prior to the onset of any obvious vesiculation or rhabdomere degeneration; the V_f of rhabdomere R7 that expresses UV sensitive rhodopsin (that does not absorb white light) did not change (Fig 1A,B). This reduction in rhabdomere size was accompanied by changes in the localization of Rh1, the rhodopsin isoform expressed in R1-R6. With just 12 hrs of illumination, there was an increase in the number of RLVs in the cell body (Fig 1C,D) A subset of these RLVs co-localize with the early and late endocytic compartment markers Rab5 and Rab7 respectively (Fig 1E,F). Over a period of 4 days, illumination results in a reduction in total Rh1 protein levels (Fig 1G) and manifests functionally as a reduction in sensitivity to light (Fig 1H).

dPLD is required to support rhabdomere volume during illumination

We generated loss-of-function mutants in *dPLD* using homologous recombination (Gong and Golic, 2003) (Figure 2-figure supplement 1A). Multiple alleles were isolated of which $dPLD^{3.1}$ is described in detail. To test if $dPLD^{3.1}$ represents an animal with no residual PLD activity, we used the transphosphatidylation assay that exploits the ability of PLD to use primary alcohols as nucleophilic acceptor. Flies were starved for 12 hrs, allowed to feed for 6 hrs on 10% ethanol/sucrose and the formation of phosphatidylethanol (PEth) monitored using LC-MS (Wakelam et al., 2007). Under these conditions, multiple species of PEth were detected in wild type flies, no PEth could be detected in $dPLD^{3.1}$ extracts under the equivalent conditions (Figure 2-fIgure supplement 1C,D). Thus $dPLD^{3.1}$ mutants have no residual PLD activity.

$dPLD^{3.1}$ flies are homozygous viable as adults. At eclosion, photoreceptor ultrastructure in $dPLD^{3.1}$ was indistinguishable from controls (Fig 2A). Following exposure to 2000 lux white light for 48 hrs, as expected, V_f occupied by peripheral rhabdomeres was reduced in wild type flies (Fig 2B) whereas V_f of R7 was unaffected. In $dPLD^{3.1}$, rhabdomere V_f reduced following illumination (Fig 2B); however, the reduction was substantially greater than in wild type (Fig 2C).

We visualized RLVs in photoreceptors by Rh1 immunolabelling and counted them. These analyses were done at 0 days post-eclosion, prior to the onset of any obvious ultrastructural change in $dPLD^{3.1}$. In dark-reared flies, the number of RLVs in $dPLD^{3.1}$ was greater than in wild type photoreceptors (Fig 2D,E). Following illumination for 12 hrs, the number of RLVs increases in both controls and $dPLD^{3.1}$; however the increase was greater in $dPLD^{3.1}$ (Fig 2E). Further, while the number of RLVs that are also Rab5-positive were not significantly different

between controls and *dPLD*$^{3.1}$, the numbers of Rab7-positive RLVs were significantly greater in *dPLD*$^{3.1}$ compared to controls (Fig 2F). Thus, during illumination there is enhanced accumulation of RLVs in a Rab7 compartment in *dPLD*$^{3.1}$.

We measured Rh1 protein levels using Western blotting in flies exposed to bright illumination for four days post-eclosion. As expected, levels of Rh1 decreased when wild type flies were reared in bright light compared to dark-reared controls (Fig 2G). In dark reared flies, Rh1 levels are equivalent in controls and *dPLD*$^{3.1}$ (Fig 2G); following illumination Rh1 levels decrease in both genotypes but the reduction seen in *dPLD*$^{3.1}$ is much greater than in wild type flies of matched eye color (Fig 2G,H). Consistent with this, we found that *dPLD*$^{3.1}$ photoreceptors were less sensitive to light compared to controls of matched eye color on eclosion (Fig 2J). These findings demonstrate that during illumination, the turnover of Rh1, an apical membrane protein of photoreceptors is altered in *dPLD*$^{3.1}$. However, such changes were not seen in the levels or localization of TRP and NORPA, two other apical membrane proteins, during illumination (Figure 2-figure supplement 2A,B). *dPLD*$^{3.1}$ photoreceptors did not exhibit a primary defect in the electrical response to light in electroretinograms (Fig 2I, Figure 2 supplement 3 A-D).

Retinal degeneration in *dPLD*$^{3.1}$ is dependent on altered PA levels

We grew flies in constant illumination following eclosion. Under these conditions, control photoreceptors maintain normal structure; however *dPLD*$^{3.1}$ undergoes light-dependent retinal degeneration. The degeneration starts by day 5 post-eclosion and all six peripheral photoreceptors degenerate by day 14 (Fig 3A, B). This degeneration is strictly dependent on illumination as *dPLD*$^{3.1}$ not exposed to light retains normal ultrastructure up to day 14 (Fig

3A,B). Photoreceptor degeneration is underpinned by a collapse of the apical microvillar membrane as well as the accumulation of membranous whorls within the cell body (Fig 3C). Retinal degeneration was also seen in a trans-heterozygote combination of two independently isolated alleles $dPLD^{3.1}$ and $dPLD^{3.3}$ (Figure 3 supplement1A, B). No degeneration was seen in either $dPLD^{3.1}$/+ or $dPLD^{3.3}$/+ (Figure 3 supplement 1A) excluding a dominant negative or neomorphic effect of these alleles. The light dependent degeneration was also seen when the $dPLD^{3.1}$ allele was placed over a deficiency chromosome for the *dPLD* gene region; in $dPLD^{3.1}$*/Df(2R)ED1612*, retinal degeneration was comparable and was no worse than in $dPLD^{3.1}$ homozygotes (Figure 3 supplement 1C), suggesting that $dPLD^{3.1}$ is a null allele. Light-dependent degeneration in $dPLD^{3.1}$ could be rescued by a wild type transgene [$dPLD^{3.1}$*;Hs>dPLD*] but not by a lipase dead transgene [$dPLD^{3.1}$*;Hs>*$dPLD^{K/R}$] (Fig 3D,E, F).These results demonstrate that dPLD enzyme activity is required to support normal photoreceptor ultrastructure during illumination.

In order to understand the biochemical basis of retinal degeneration of $dPLD^{3.1}$, we measured levels of PC and PA from retinal extracts using direct infusion mass spectrometry (Schwudke et al., 2011). We found that levels of PC were not significantly different between controls and $dPLD^{3.1}$ (Fig 4A). By contrast, there was a significant decrease in total PA levels in $dPLD^{3.1}$ (Fig 4B). At the level of molecular species, this reduction was associated with changes in the levels of PA species with longer acyl chain lengths (Fig 4C). Rescue of retinal degeneration in $dPLD^{3.1}$ by reconstitution with *Hs>dPLD* was associated with restoration in PA levels back to that of controls (Fig 4D). Reconstitution with *Hs>*$dPLD^{K/R}$ that failed to rescue degeneration also did not restore PA levels in $dPLD^{3.1}$ (Fig 4D). These results show that retinal degeneration in $dPLD^{3.1}$ is correlated with reduced PA levels.

We hypothesized that if the retinal degeneration in *dPLD*$^{3.1}$ is due to reduced PA levels, elevating PA levels in *dPLD*$^{3.1}$ retinae by methods independent of dPLD activity should rescue this phenotype. It is reported that in *laza*^{22} photoreceptors lacking Type II PA phosphatase activity, PA levels rise during exposure to light (Garcia-Murillas et al., 2006). We generated double mutants *dPLD*$^{3.1}$*;laza*^{22} and studied retinal degeneration in these flies. We found that *dPLD*$^{3.1}$*;laza*^{22} photoreceptors did not undergo light dependent-degeneration (Fig 4E). To test if this was due to restoration of PA levels we measured PA levels in all these genotypes. As previously reported, we found that PA levels were elevated in *laza*^{22}; importantly the reduced levels of PA seen in *dPLD*$^{3.1}$ was restored in *dPLD*$^{3.1}$*;laza*^{22} (Fig 4F). We also overexpressed *rdgA*, encoding the major diacylglycerol kinase activity in photoreceptors. Overexpression of *rdgA* has previously been shown to elevate PA levels without affecting retinal ultrastructure (Raghu et al., 2009). When *rdgA* is overexpressed in *dPLD*$^{3.1}$ (*dPLD*$^{3.1}$*;Rh1>rdgA*), retinal degeneration was completely rescued and the reduced PA levels seen in *dPLD*$^{3.1}$ were reverted back to wild type levels (Figure 4-figure supplement 1A,B). Collectively, these observations suggest that reduced PA levels underlie the retinal degeneration phenotype of *dPLD*$^{3.1}$.

Illumination-dependent dPLD activity regulates PA levels and Rh1 turnover.

The finding that *dPLD*$^{3.1}$ undergoes light-dependent retinal degeneration suggests that *dPLD* might be activated during illumination. When *Drosophila* photoreceptors are illuminated, a key source of PA is the sequential activity of PLCβ and DGK (Inoue et al., 1989; Yoshioka et al., 1983) and PA is also metabolized by the PA phosphatase *laza* (Garcia-Murillas et al., 2006). In order to uncover a potential *dPLD* generated pool of PA, we exploited *dGq*^{1} mutants in which the failure to activate PLCβ results in a suppression of PA production via DGK (Garcia-Murillas

et al., 2006). We compared PA levels in retinal extracts from dGq^{1} with dGq^{1},$dPLD^{3.1}$ both in the dark and following illumination with 12 hrs of light. PA levels from both genotypes were comparable in dark reared flies; however, PA levels rise in dGq^{1} mutants following illumination presumably reflecting production from a non-PLCβ-DGK source (Fig 4G). This rise in PA levels was suppressed in dGq^{1}, $dPLD^{3.1}$ flies (Fig 4G). Thus illumination induces *dPLD* dependent PA production in *Drosophila* photoreceptors.

dPLD was overexpressed in adult photoreceptors (*Rh1>dPLD*). Following 12 hrs of white light illumination, the number of RLVs increases in the cell body of wild type (Fig 4H,I). However in *Rh1>dPLD* the number of RLVs did not increase (Fig 4H,I); this effect was not seen on overexpression of $Rh1>dPLD^{K/R}$ (Fig 4H,I) suggesting that the ability of *dPLD* to regulate RLV turnover is dependent on its catalytic activity. Together, these observations suggest that during illumination *dPLD* activity can support RLVs turnover.

dPLD activity supports RLV removal from the cell body during illumination

RLV numbers in the cell body are an outcome of the balance between ongoing clathrin-dependent endocytosis of Rh1 containing rhabdomere membrane as well as mechanisms that remove these from the cell body. To understand the mechanism underlying the increased RLV number in $dPLD^{3.1}$, we exploited the temperature-sensitive allele of dynamin, shi^{ts1}. At the permissive temperature of 18^{0}C, where dynamin function is normal, we exposed flies to a 5 min pulse of bright white light to trigger Rh1 isomerization to M and trigger its endocytosis. Under these conditions, the number of RLVs generated in cells with and without PLD function was indistinguishable (Fig 5A,B). Following this, animals were rapidly shifted to 25^{0}C,

incubated for various time periods, retinae were fixed, processed and RLVs counted. Under these conditions, in *shi*^{ts1}, where there is no further ongoing endocytosis, RLV numbers fall rapidly, presumably reflecting the removal of previously endocytosed vesicles (Fig 5A). By contrast, in *shi*^{ts1}*;dPLD*$^{3.1}$, following the shift to 25^{0}C post-illumination, there was no drop in RLV number with time implying a defect in mechanisms that remove RLVs from the cell body (Fig 5B).

We counted RLVs in *norpA*^{P24} subjected to bright illumination; as previously reported, we found RLV numbers were elevated (Chinchore et al., 2009). This elevation in RLV number could be suppressed by the overexpression of *dPLD* (Fig 5C,D). We also found that the light-dependent retinal degeneration in *norpA*^{P24} that is reported to depend on RLV accumulation in a Rab7 compartment (Chinchore et al., 2009)(Wang et al., 2014) could be partially suppressed by overexpressing *dPLD* (Fig 5E,F). Interestingly, we found that during illumination, in *Rh1>dPLD*, there was a significant reduction in the number of Rab7-positive RLVs but not in the number of Rab5-positive RLVs. Collectively, these findings show that *dPLD* supports a process that can clear RLVs from the cell body of photoreceptors during illumination.

dPLD regulates clearance of RLVs via retromer function

The retromer complex plays a central role in removing endocytosed transmembrane proteins from the lysosomal pathway and targets them to other cellular compartments (Gallon and Cullen, 2015). We tested the effect of manipulating core members of the retromer complex in photoreceptors. RNAi downregulation of *vps35* results in an increase in RLV numbers both in the dark and following 12hr illumination (Fig 6 A, B). We tested the effect of overexpressing

243 *vps35* in photoreceptors during illumination; in an otherwise wild type fly, this did not result in
244 changes in RLV number (Fig 6D) or caused retinal degeneration (Fig 6C). However in $dPLD^{3.1}$
245 photoreceptors, overexpression of *vps35* results in two key outcomes: (i) the increased
246 numbers of RLVs seen in $dPLD^{3.1}$ were reduced back to wild type levels (Fig 6D) and (ii) the
247 retinal degeneration of $dPLD^{3.1}$ is suppressed (Fig 6C).
248
249 During illumination, overexpression of *dPLD* results in a reduction of RLV number in a lipase
250 dependent manner (Fig4H,I). We tested the requirement of intact retromer function for the
251 ability of *dPLD* to clear RLVs. We found that in cells where *vps35* was downregulated,
252 overexpression of *dPLD* could not reduce RLV numbers (Fig 6E,F). These findings suggest
253 that intact retromer function is required for *dPLD* to support the clearance of RLVs during
254 illumination.
255
256 **Overexpression of *garz* rescues retinal degeneration in $dPLD^{3.1}$**
257 We overexpressed *garz*, the *Drosophila* ortholog of the guanine nucleotide exchange factor
258 (GBF1) of Arf1 (Cox et al., 2004). In adult photoreceptors, *garz* overexpression does not
259 impact rhabdomere structure during illumination (Fig 7B,C) although RLV numbers were
260 reduced (Fig 7A). When *garz* is overexpressed in $dPLD^{3.1}$, it completely rescues retinal
261 degeneration (Fig 7B,C). These findings strongly suggest that retinal degeneration in $dPLD^{3.1}$
262 may be due to reduced ARF1 activity. If this model is true then reducing *garz* activity in wild
263 type flies should phenocopy $dPLD^{3.1}$. To test this we down regulated *garz* in photoreceptors;
264 this resulted in light-dependent retinal degeneration, the kinetics of which were comparable to

that of *dPLD*$^{3.1}$ (Fig 7D,E). Finally we found that overexpression of *garz* reduced RLV number in *dPLD*$^{3.1}$ back towards wild type controls (Fig 7F).

dPLD and _garz_ are required for RLV clearance during illumination

Since both *garz* and *dPLD* play a role in RLV clearance during illumination (Fig 7 and Fig 4), we tested the requirement of each molecule on the other for this function. We found that the ability of Rh1>dPLD to clear RLVs required intact *garz* function. When *garz* is also depleted (*Rh1>garz*^{RNAi}) in *Rh1>dPLD* cells , the reduction in RLV number seen in *Rh1>dPLD* alone was attenuated (Fig 8 A). This finding suggests that a *garz* dependent step is required to support RLV clearance by dPLD during illumination.

We also explored the route by which *garz* activity clears RLVs. When *Rh1>garz* is performed in photoreceptors where retromer function is depleted (*Rh1>vps35*^{RNAi}), the reduction in RLV number seen in *Rh1>garz* alone is substantially blocked (Fig 8B). Thus the ability of *garz* to support RLV clearance from the cell body requires intact retromer function.

Since our observations indicate a role of dPLD and its product PA in the context of Arf1-GTP activity, we tested the requirement for dPLD in regulating the biological activity of Arf1. In photoreceptors, overexpression of constitutively active Arf1, Arf1^{CA} (*Rh1>Arf1*^{CA}), results in ultrastructure defects in the rhabdomere (Fig 8C). We expressed *Rh1>Arf1*^{CA} in *dPLD*$^{3.1}$ and studied its effect on ultrastructure. In the absence of dPLD function the effect of *Rh1>Arf1*^{CA} on ultrastructure was substantially reduced (Fig 8C iii versus iv). This finding suggests that PA produced by dPLD is required to mediate the effects of Arf1 *in vivo*.

Discussion

Although the importance of plasma membrane turnover in determining cellular responses to external stimuli is well appreciated, the mechanisms that regulate this process remain unclear. In photoreceptors, change in size of photosensitive membranes during illumination represents a special example of the broad principle of plasma membrane turnover following receptor-ligand interaction. In *dPLD*$^{3.1}$ photoreceptors, the process of light-induced membrane turnover is exaggerated; these photoreceptors show larger reductions in rhabdomere volume and greater reductions in Rh1 levels than is seen in wild type flies. The physiological consequence of this is that *dPLD*$^{3.1}$ photoreceptors are less sensitive to light than controls when reared in light (Fig 2J).

During illumination, RLVs are generated and mature through Rab5 and Rab7 endocytic compartments. We found that (i) photoreceptors contain a light-stimulated PLD activity, (ii) Loss of dPLD activity results in enhanced numbers of Rab7-positive RLVs in the cell body during illumination, (iii) overexpression of catalytically active dPLD was able to clear light-induced Rab7-positive RLVs in wild type cells and (iv) dPLD overexpression was able to reduce the enhanced RLV number and partially suppress retinal degeneration in *norpA*^{P24}, a mutant that shows enhanced Rab7 positive RLVs during illumination. Thus dPLD represents an enzyme activity that couples the generation of RLVs by light-induced endocytosis to their removal from the cell body. It has previously been reported that the Rh1 that accumulates in Rab7 compartment is targeted for degradation thus leading to retinal degeneration (Chinchore et al., 2009). Accumulation of Rh1 in Rab7 positive endosomes may explain the progressive microvillar collapse and reduced Rh1 protein levels in the cell body of *dPLD*$^{3.1}$. Both, the microvillar degeneration and reduced PA levels of *dPLD*$^{3.1}$ retinae were rescued by a *dPLD*

311 transgene with intact lipase activity and elevation of PA levels was sufficient to rescue this
312 phenotype. Collectively, our observations strongly suggest that photoreceptors depend on a
313 light-activated *dPLD* to generate PA to maintain apical membrane turnover during illumination.
314 They also suggest that protein-protein interactions of PLD, independent of its catalytic activity,
315 may not be a primary mechanism underlying the function of this enzyme in cells.

316 In principle, the number of RLVs seen in a photoreceptor following illumination is a balance
317 between ongoing endocytosis and processes that remove endocytosed RLVs either by
318 recycling to the microvillar membrane or targeting to the late endosome-lysosome system for
319 degradation. Using the temperature sensitive allele of dynamin shi^{ts1}, we were able to
320 uncouple RLV endocytosis from their removal from the cell body and found that the generation
321 of RLVs during illumination was not dependent on *dPLD* activity (Fig 5I) and the number of
322 Rab5-positive RLVs was not increased in $dPLD^{3.1}$ photoreceptors (Fig 2F). Collectively, these
323 observations suggest no primary defect in clathrin dependent endocytosis in $dPLD^{3.1}$.
324 However, we found that in $dPLD^{3.1}$, the clearance of endocytosed RLVs was dramatically
325 slower than in controls implying that dPLD supports a process that clears RLVs from the cell
326 body. These RLVs were Rab7-positive suggesting that they accumulate in late endosomes.
327 Conversely, in *Rh1>dPLD*, the number of Rab7-positive RLVs was fewer than in wild type
328 cells. Together these observations strongly suggest that *dPLD* activity supports a process that
329 clears RLVs post endocytosis.
330
331 Following endocytosis, endosomes containing trans-membrane proteins (such as Rh1) can be
332 targeted for lysosomal degradation or be retrieved for recycling to other membranes through
333 retromer-dependent processes. The enhanced RLV numbers as well as retinal degeneration in

334 *dPLD*$^{3.1}$ could be rescued by enhancing retromer activity and the ability of *dPLD*
335 overexpression to reduce RLV number during illumination required intact retromer activity.
336 Together these observations suggest that during illumination *dPLD* stimulates RLV clearance
337 through a retromer-dependent mechanism. We found enhanced number of Rab7 positive
338 RLVs in *dPLD*$^{3.1}$ and *Rh1>dPLD* had reduced number of Rab7 positive RLVs. A previous study
339 has reported that retromer activity can clear RLVs from a Rab7 positive compartment (Wang et
340 al., 2014). Together our findings suggest that in the absence of dPLD the sorting of RLVs away
341 from Rab7 endosomes into retromer-dependent recycling is inefficient.
342
343 Why might cargo sorting in *dPLD*$^{3.1}$ be abnormal ? Sorting reactions in vesicular transport often
344 involve a small GTPase working in conjunction with a lipid-metabolizing enzyme. Altering *garz*
345 function, presumably altering Arf1-GTP levels, has three consequences: (i) in wild type cells,
346 enhancing *garz* levels results in fewer RLVs and blocks the rise in RLVs seen during light
347 exposure. (ii) enhancing *garz* levels reduces RLV accumulation in *dPLD*$^{3.1}$ (iii) enhancing *garz*
348 levels suppresses degeneration in *dPLD*$^{3.1}$ while depleting *garz* in wild type flies results in light-
349 dependent retinal degeneration with a time course similar to that seen in *dPLD*$^{3.1}$. Thus an
350 Arf1-GTP dependent step is required for both RLV turnover and maintaining apical domain
351 size in photoreceptors. Our finding that the ability of *Rh1>dPLD* to modulate RLV number
352 requires intact *garz* function (Fig 8A) is consistent with this model. These findings imply that
353 Arf1-GTP levels positively regulate a step that enhances RLV recycling to the microvillar
354 plasma membrane in the face of ongoing light-induced endocytosis, presumably through
355 retromer complex activity. In support of this idea, we found that the ability of *Rh1>garz* to
356 reduce RLV numbers during illumination depends on intact retromer function (Fig 8B). We

propose, that during illumination, rhabdomere size is maintained by the balance between clathrin-dependent endocytosis generating RLVs and an Arf1-GTP dependent sorting event that recycles RLVs to the plasma membrane via retromer activity (Fig 8D). *dPLD*, specifically its product PA is likely able to balance these two reactions by coupling light induced endocytosis to Arf1-dependent sorting of RLVs into the recycling pathway. Previous studies have identified proteins from brain cytosol that bind PA *in vitro* and are known to regulate membrane transport events; prominent among these was Arf1 (Manifava et al., 2001) although the *in vivo* significance of this binding is unknown. Our findings that the biological activity of $Arf1^{CA}$ in photoreceptors requires intact *dPLD* activity and that the ability of increased *garz* (Arf1-GEF) levels to clear RLVs requires intact *dPLD* function suggests that Arf1 is a key target of PA generated by dPLD in mediating sorting and recycling of RLVs in photoreceptors. It has been reported that EHD1 an ATPase required to generate tubular recycling endosomes is recruited by MICAL-L1 and the BAR domain protein syndapin2 both of which bind PA (Giridharan et al., 2013). It is possible that these proteins are also targets of PA generated by dPLD. In the absence of PA, RLV sorting into the recycling pathway is impaired in $dPLD^{3.1}$, some fraction of the endocytosed RLVs accumulates in Rab7 endosomes and is targeted for degradation leading to the reduction in Rh1 levels. These reduced Rh1 levels likely account for the reduced light sensitivity of dPLD mutants reported both in this study as well as in a previous analysis (Lalonde et al., 2005).

What is the transduction pathway between photon absorption and dPLD activation? $dPLD^{3.1}$ photoreceptors show normal electrical responses to light and the microvillar degeneration of $dPLD^{3.1}$ could not be suppressed by a strong hypmorph of *dGq* (Scott et al., 1995) that is

required for PLCβ dependent phototransduction. We also found that light-activated elevation of PA levels was dependent on dPLD activity but did not require Gq-PLCβ signalling. Collectively these findings imply that *dPLD* activity is dispensable for Gq-PLCβ mediated activation of TRP channels and that the light-dependent degeneration of $dPLD^{3.1}$ is not a consequence of abnormal TRP channel activation.

Our findings suggest that M activates *dPLD* without the requirement of Gq function although the molecular mechanism remains to be determined. *dPLD* has been reported to be localized in the submicrovillar cisternae (Lalonde et al., 2005; Raghu et al., 2009), a specialization of the smooth endoplasmic reticulum that is positioned ca. 10 nm from the plasma membrane at the base of the microvilli (Yadav et al., 2016). At this location, *dPLD* might bind to the C-terminal tail of M either before or after it is endocytosed into RLV; binding of mammalian PLD1 has been reported to the C-terminal tail of several rhodopsin superfamily GPCRs including the 5-$HT2_a$, muscarinic and opioid receptors [(Barclay et al., 2011) and references therein]. It is possible that PA produced by *dPLD* bound to the C-terminus of Rh1 may then stimulate recycling to the apical membrane. Thus the control of apical membrane turn over by *dPLD* during illumination may represent an example by which ligand bound GPCRs signal without a direct involvement for heterotrimeric G-protein activity. More generally, in the brain neurons and glial cells express GPCRs (5-HT2a, mGluR and opioid receptors) of key functional importance. Controlling these GPCR numbers on the plasma membrane during receptor stimulation (of which rhodopsin turnover during illumination is a prototypical example) is of critical importance to brain function and mechanisms that regulate this process will likely be crucial for the understanding and treatment of neuropsychiatric syndromes.

Materials and methods

Fly cultures and Stocks: Flies were reared on medium containing corn flour, sugar, yeast powder and agar along with antibacterial and antifungal agents. Flies were maintained at 25°C and 50% relative humidity. There was no internal illumination within the incubator and the flies were subjected to light pulses of short duration only when the incubator door was opened. When required, flies were grown in an incubator with constant illumination from a white light source (intensity ~2000 lux).

The wild type used for all experiments was Red Oregon-R. GAL4-UAS system was used to drive expression of transgenic constructs. The following transgenic lines were obtained from the Bloomington Stock Center: UAS-GFP::Rab5 (B#43336),UAS-YFP::Rab7 (B#23270). UAS-*garz*^{RNAi} (V# 42140) was obtained from the Vienna Drosophila RNAi Center. Dicer;UAS-vps35^{RNAi} was obtained from Miklós Sass (Eötvös Loránd University, Budapest, Hungary) and UAS-vps35::HA was obtained from Prof. Hugo Bellen (Baylor College of Medicine, Howard Hughes Medical Institute, Houston).

Optical Neutralization and Scoring Retinal Degeneration: Flies were cooled on ice, decapitated using a sharp blade, and fixed on a glass slide using a drop of colorless nail varnish. Imaging was done using 40X oil objective of Olympus BX43 microscope. In order to obtain a quantitative index of degeneration, atleast five flies were scored for each time point. A total of 50 ommatidia were assessed to generate degeneration index. To quantify degeneration, a score of 1 was assigned to each rhabdomere that appeared to be wild type.

Thus wild type ommatidia will have a score of 7. Mutants undergoing degeneration will have a score between 1 and 7. Score were expressed as mean ± SEM.

Electroretinograms: Flies were anesthetized on ice and immobilized at the end of a disposable pipette tip using a drop of nail varnish. The recording electrode (GC 100F-10 borosilicate glass capillaries, 1mm O.D and 0.58mm I.D from Harvard apparatus filled with 0.8% w/v NaCl solution) was placed on the surface of eye and the reference electrode was placed on the neck region/thorax. Flies were dark adapted for 5 min followed by ten repeated green light flashes of 2s duration, each after an interval of 10 seconds. Stimulating light was delivered from a LED light source placed within a distance of 5 mm of the fly's eye through a fiber optic guide. Calibrated neutral density filters were used to vary the intensity of the light over 5 log units. Voltage changes were amplified using a DAM50 amplifier (WPI) and recorded using pCLAMP 10.2. Analysis of traces was performed using Clampfit (Axon Laboratories).

Western blotting: Heads from one day old flies (unless otherwise specified) were decapitated in 2X SDS-PAGE sample buffer followed by boiling at 95^{o}C for 5 minutes. For detection of rhodopsin, samples were incubated at 37^{0}C for 30 minutes and then subjected to SDS-PAGE and western blotting. The following antibodies were used: anti-rhodopsin (1:250-4C5), anti-α-tubulin (1:4000,E7c), anti-TRP (1:4000) and anti-NORPA (1:1000). All secondary antibodies (Jackson Immunochemicals) were used at 1:10000 dilution. Quantification of the blot was done using Image J software from NIH (Bethesda, MD, USA).

Immunohistochemistry: For immunofluorescence studies retinae from flies were dissected under low red light in phosphate buffer saline (PBS). Retinae were fixed in 4% paraformaldehyde in PBS with 1 mg/ml saponin at room temperature for 30 minutes. Fixed

eyes were washed 3 times in PBST (1X PBS+0.3% TritonX-100) for 10 minutes. The sample was then blocked in a blocking solution (5% Fetal Bovine Serum in PBST) for 2 hours at room temperature, after which the sample was incubated with primary antibody in blocking solution overnight at 4^{o}C on a shaker. The following antibodies were used: anti-Rh1 (1:50),anti-TRP (1:250) and anti-GFP (1:5000,abcam [ab13970]). Appropriate secondary antibodies conjugated with a fluorophore were used at 1:300 dilutions [Alexa Fluor 488/568/633 IgG, (Molecular Probes)] and incubated for 4 hrs at room temperature. Wherever required, during the incubation with secondary antibody, Alexa Fluor 568-phalloidin (Invitrogen) was also added to the tissues to stain the F-actin. After three washes in PBST, sample was mounted in 70% glycerol in 1X PBS. Whole mounted preps were imaged on Olympus FV1000 confocal microscope using Plan-Apochromat 60x,NA 1.4 objective (Olympus).

Rhodopsin loaded vesicles (RLV's) counting: Whole mount preparations of photoreceptors stained with anti-Rh1 were imaged on Olympus FV1000 confocal microscope using Plan-Apochromat 60X, NA 1.4 objective (Olympus). The RLV's per ommatidium were counted manually across the Z-stacks using Image J software from NIH (Bethesda, MD, USA).

Electron microscopy and Volume fraction analysis: Samples for TEM were prepared as mentioned in previous publication (Garcia-Murillas et.al,2006). Briefly samples were bisected in ice cold fixative solution (For 1ml: 0.5ml of 0.2 M PIPES (pH:7.4),80µl of 25% EM grade glutaraldehyde, 10 µl of 30% H_2O_2 and 0.41ml water). After over-night fixation at 4^{0}C, samples were washed in 0.1M PIPES (thrice 10 min. each) and then fixed in 1% osmium tetroxide (15 mg Potassium Ferrocyanide, 500 µl 0.2M PIPES, 250 ul 4% Osmium tetroxide and 250 µl of distilled water) for 30 min. The eyes were then washed with 0.1M PIPES (thrice 10 min. each)

and then stained in en-block (2% Uranyl acetate) for 1 hour. Eyes were dehydrated in ethanol series and embedded in epoxy. Ultrathin sections (60 nm) were cut and imaged on a Tecnai G2 Spirit Bio-TWIN (FEI) electron microscope.

For volume fraction analysis TEM images of *Drosophila* retinae were acquired and analyzed using the ADCIS Stereology toolkit 4.2.0 from the Aperio Imagescope suite. A grid probe was used whose probe intersections were accurate to about 200-300 points. The volume fraction (V_f) of the rhabdomere with respect to its corresponding photoreceptor cell was calculated as:

$$V_f = \frac{\text{Number of points falling on the rhabdomere}}{\text{Total number of points on the cell}}$$

Volume fractions were calculated separately for R1-R6 and R7

Scoring Retinal Degeneration using TEM: TEM images were acquired using Tecnai G2 Spirit Bio-TWIN (FEI) electron microscope. To quantify degeneration, a score of 1 was assigned to each rhabdomere that appeared to be wild type and a score of 0.5 was assigned to each rhabdomere that appeared to be partially degenerated.

Isolation of pure retinal tissue: Pure preparations of retinal tissue were collected using previously described methods (Fujita et al., 1987). Briefly, 0 to 12-hr-old flies (unless otherwise specified) were snap frozen in liquid nitrogen and dehydrated in acetone at -80^{o}C for 48 hr. The acetone was then drained off and the retinae dried at room temperature. They were cleanly separated from the head at the level of the basement membrane using a scalpel blade.

Lipid extraction and mass spectrometry: 10 heads or 100 retinae per sample (dissected from one day old flies) were homogenized in 0.1 ml methanol containing internal standards) using an automated homogenizer. The methanolic homogenate was transferred into a screw-capped tube. Further methanol (0.3 ml) was used to wash the homogenizer and was combined in the special tube. 0.8 ml chloroform was added and left to stand for 15 min. 0.88% KCl (0.4ml) was added to split the phases. The lower organic phase containing the lipids were dried, re-suspended in 400µl of chloroform:methanol 1:2 and was ready for analysis. Total lipid phosphate was quantified from each extract prior to infusion into the mass spectrometer.

Mass spec analyses were performed on a LTQ Orbitrap XL instrument (Thermo Fisher Scientific) using direct infusion method. Stable ESI based ionisation of glycerophospholipids was achieved using a robotic nanoflow ion source TriVersa NanoMate (Advion BioSciences) using chips with the diameter of spraying nozzles of 4.1µm. The ion source was controlled by Chipsoft 8.3.1 software. Ionization voltages were +1.2kV and −1.2kV in positive and negative modes, respectively; back pressure was set at 0.95psi in both modes. The temperature of ion transfer capillary was 180°C. Acquisitions were performed at the mass resolution $R_{m/z400}$=100000. Dried total lipid extracts were re-dissolved in 400µl of chloroform:methanol 1:2. For the analysis, 60µl of samples were loaded onto 96-well plate (Eppendorf) of the TriVersa NanoMate ion source and sealed with aluminum foil. Each sample was analyzed for 20min in positive ion mode where PC was detected and quantified. This was followed by an independent acquisition in negative ion mode for 20min where PA was detected and quantified.

Lipids were identified by LipidXplorer software by matching *m/z* of their monoisotopic peaks to the corresponding elemental composition constraints. Molecular Fragmentation Query Language (MFQL) queries compiled for all the aforementioned lipid classes. Mass tolerance was 5p.p.m. and intensity threshold was set according to the noise level reported by Xcalibur software (Thermo Scientific).

Transphosphatidylation Assay: One day old flies were starved for 12 hrs and then fed on 10% ethanol in sucrose for 6 hrs. Following this lipids were extracted (with appropriate internal standards) and phosphatidylethanols detected and quantified by HPLC/MS method (Wakelam et al., 2007).

Data Analysis: Data were tested for statistics using unpaired t-test. *** denotes $p < 0.001$; ** denotes $p < 0.01$; * denotes $p < 0.05$ and ns denotes not significant

Acknowledgements: This work was supported by the National Centre for Biological Sciences-TIFR, the Biotechnology and Biological Sciences Research Council, U.K, Department of Biotechnology, Government of India and a Wellcome Trust-DBT India Alliance Senior Fellowship to PR. We thank the NCBS- Max Planck Lipid center, Electron Microscopy, Imaging (CIFF) and Fly Facility for assistance. We thank Hanneke Okkenhaug for assistance at an early stage of this project. We acknowledge the generous support of numerous colleagues who provided us with fly stocks and antibodies.

References

Abràmoff, M.D., Mullins, R.F., Lee, K., Hoffmann, J.M., Sonka, M., Critser, D.B., Stasheff, S.F., and Stone, E.M. (2013). Human photoreceptor outer segments shorten during light adaptation. Invest. Ophthalmol. Vis. Sci. *54*, 3721–3728.

Arendt, D. (2003). Evolution of eyes and photoreceptor cell types. Int. J. Dev. Biol. *47*, 563–571.

Barclay, Z., Dickson, L., Robertson, D.N., Johnson, M.S., Holland, P.J., Rosie, R., Sun, L., Fleetwood-Walker, S., Lutz, E.M., and Mitchell, R. (2011). 5-HT2A receptor signalling through phospholipase D1 associated with its C-terminal tail. Biochem. J. *436*, 651–660.

Blest, A. (1988). The turnover of phototransducive membrane in compound eyes and ocelli. In Advances in Insect Physiology, P. Evans, and V. Wigglesworth, eds. (Academic Press), pp. 1–53.

Brown, H.A., Gutowski, S., Moomaw, C.R., Slaughter, C., and Sternweis, P.C. (1993). ADP-ribosylation factor, a small GTP-dependent regulatory protein, stimulates phospholipase D activity. Cell *75*, 1137–1144.

Cai, D., Zhong, M., Wang, R., Netzer, W.J., Shields, D., Zheng, H., Sisodia, S.S., Foster, D.A., Gorelick, F.S., Xu, H., et al. (2006). Phospholipase D1 corrects impaired betaAPP trafficking and neurite outgrowth in familial Alzheimer's disease-linked presenilin-1 mutant neurons. Proc Natl Acad Sci U S A *103*, 1936–1940.

Chinchore, Y., Mitra, A., and Dolph, P.J. (2009). Accumulation of rhodopsin in late endosomes triggers photoreceptor cell degeneration. PLoS Genet. *5*, e1000377.

551 Choi, W.S., Kim, Y.M., Combs, C., Frohman, M.A., and Beaven, M.A. (2002). Phospholipases
552 D1 and D2 regulate different phases of exocytosis in mast cells. J.Immunol *168*, 5682–5689.

553 Cockcroft, S., Thomas, G.M., Fensome, A., Geny, B., Cunningham, E., Gout, I., Hiles, I., Totty,
554 N.F., Truong, O., and Hsuan, J.J. (1994). Phospholipase D: a downstream effector of ARF in
555 granulocytes. Science (80-.). *263*, 523–526.

556 Cockcroft, S., Way, G., O'Luanaigh, N., Pardo, R., Sarri, E., and Fensome, A. (2002).
557 Signalling role for ARF and phospholipase D in mast cell exocytosis stimulated by crosslinking
558 of the high affinity FcepsilonR1 receptor. Mol Immunol *38*, 1277–1282.

559 Cox, R., Mason-Gamer, R.J., Jackson, C.L., and Segev, N. (2004). Phylogenetic analysis of
560 Sec7-domain-containing Arf nucleotide exchangers. Mol Biol Cell *15*, 1487–1505.

561 Gallon, M., and Cullen, P.J. (2015). Retromer and sorting nexins in endosomal sorting.
562 Biochem. Soc. Trans. *43*, 33–47.

563 Garcia-Murillas, I., Pettitt, T., Macdonald, E., Okkenhaug, H., Georgiev, P., Trivedi, D.,
564 Hassan, B., Wakelam, M., and Raghu, P. (2006). lazaro encodes a lipid phosphate
565 phosphohydrolase that regulates phosphatidylinositol turnover during Drosophila
566 phototransduction. Neuron *49*, 533–546.

567 Giridharan, S.S.P., Cai, B., Vitale, N., Naslavsky, N., and Caplan, S. (2013). Cooperation of
568 MICAL-L1, syndapin2, and phosphatidic acid in tubular recycling endosome biogenesis. Mol.
569 Biol. Cell *24*, 1776–1790, S1-15.

570 Gong, W.J., and Golic, K.G. (2003). Ends-out, or replacement, gene targeting in Drosophila.
571 Proc Natl Acad Sci U S A *100*, 2556–2561.

572 Hardie, R.C., and Raghu, P. (2001). Visual transduction in Drosophila. Nature *413*, 186–93.

573 Huang, P., Altshuller, Y.M., Hou, J.C., Pessin, J.E., and Frohman, M.A. (2005). Insulin-
574 stimulated plasma membrane fusion of Glut4 glucose transporter-containing vesicles is
575 regulated by phospholipase D1. Mol Biol Cell *16*, 2614–2623.

576 Inoue, H., Yoshioka, T., and Hotta, Y. (1989). Diacylglycerol Kinase Defect In a Drosophila
577 Retinal Degeneration Mutant Rdga. *264*, 5996–6000.

578 Lalonde, M.M., Janssens, H., Rosenbaum, E., Choi, S.Y., Gergen, J.P., Colley, N.J., Stark,
579 W.S., and Frohman, M.A. (2005). Regulation of phototransduction responsiveness and retinal
580 degeneration by a phospholipase D-generated signaling lipid. J Cell Biol *169*, 471–479.

581 LaVail, M.M. (1976). Rod outer segment disc shedding in relation to cyclic lighting. Exp. Eye
582 Res. *23*, 277–280.

583 De Los Santos, P., and Neiman, A. (2004). Positive and negative regulation of a SNARE
584 protein by control of intracellular localization. Mol Biol Cell 1802–1815.

585 Manifava, M., Thuring, J.W., Lim, Z.Y., Packman, L., Holmes, A.B., and Ktistakis, N.T. (2001).
586 Differential binding of traffic-related proteins to phosphatidic acid- or phosphatidylinositol (4,5)-
587 bisphosphate-coupled affinity reagents. J.Biol.Chem *276*, 8987–8994.

588 Nakanishi, H., Morishita, M., Schwartz, C.L., Coluccio, A., Engebrecht, J., and Neiman, A.M.
589 (2006). Phospholipase D and the SNARE Sso1p are necessary for vesicle fusion during
590 sporulation in yeast. J Cell Sci *119*, 1406–1415.

591 Raghu, P., Coessens, E., Manifava, M., Georgiev, P., Pettitt, T., Wood, E., Garcia-Murillas, I.,
592 Okkenhaug, H., Trivedi, D., Zhang, Q., et al. (2009). Rhabdomere biogenesis in Drosophila

photoreceptors is acutely sensitive to phosphatidic acid levels. J Cell Biol *185*, 129–145.

Raghu, P., Yadav, S., and Mallampati, N.B.N. (2012). Lipid signaling in Drosophila photoreceptors. Biochim. Biophys. Acta *1821*, 1154–1165.

Rudge, S.A., Pettitt, T.R., Zhou, C., Wakelam, M.J., and Engebrecht, J.A. (2001). SPO14 separation-of-function mutations define unique roles for phospholipase D in secretion and cellular differentiation in Saccharomyces cerevisiae. Genetics *158*, 1431–1444.

Schwudke, D., Schuhmann, K., Herzog, R., Bornstein, S.R., and Shevchenko, A. (2011). Shotgun lipidomics on high resolution mass spectrometers. Cold Spring Harb Perspect Biol *3*, a004614.

Scott, K., Becker, A., Sun, Y., Hardy, R., and Zuker, C. (1995). Gq alpha protein function in vivo: genetic dissection of its role in photoreceptor cell physiology. Neuron *15*, 919–927.

Vitale, N., Caumont, A.S., Chasserot-Golaz, S., Du, G., Wu, S., Sciorra, V.A., Morris, A.J., Frohman, M.A., and Bader, M.F. (2001). Phospholipase D1: a key factor for the exocytotic machinery in neuroendocrine cells. EMBO J *20*, 2424–2434.

Wakelam, M.J.O., Pettitt, T.R., and Postle, A.D. (2007). Lipidomic analysis of signaling pathways. Methods Enzymol. *432*, 233–246.

Wang, S., Tan, K.L., Agosto, M.A., Xiong, B., Yamamoto, S., Sandoval, H., Jaiswal, M., Bayat, V., Zhang, K., Charng, W.-L., et al. (2014). The retromer complex is required for rhodopsin recycling and its loss leads to photoreceptor degeneration. PLoS Biol. *12*, e1001847.

White, R.H., and Lord, E. (1975). Diminution and enlargement of the mosquito rhabdom in light and darkness. J. Gen. Physiol. *65*, 583–598.

614 Xiong, B., and Bellen, H.J. (2013). Rhodopsin homeostasis and retinal degeneration: lessons
615 from the fly. Trends Neurosci. *36*, 652–660.

616 Yadav, S., Cockcroft, S., and Raghu, P. (2016). The Drosophila photoreceptor as a model
617 system for studying signalling at membrane contact sites. Biochem. Soc. Trans. *44*, 447–451.

618 Yoshioka, T., Inoue, H., and Hotta, Y. (1983). Defective phospholipid metabolism in the
619 retinular cell membrane of norpA (no receptor potential) visual transduction mutants of
620 Drosophila. Biochem. Biophys. Res. Commun. *111*, 567–573.

621

622

623

624

625

626

627

628

629

630

631

632

Figure Legends

Figure 1: Rhabdomere size regulation during illumination in *Drosophila* photoreceptors

A. TEM images of single rhabdomere from wild type photoreceptors (PRs) of 2 day old flies post eclosion reared in constant dark (CD), 12 hour light, 12 hour dark (12h L/D) and constant light (CL). Scale bar: 1 µm.

B. Quantification of rhabdomere volume in PRs reared in various conditions. The peripheral PRs represent R1 to R6 rhabdomeres. The X-axis represents the rearing condition and the Y-axis represents the volume fraction (V_f) of rhabdomere expressed as a % with respect to total cell volume. n=90 rhabdomeres taken from three separate flies.

C. Longitudinal section (LS) of retinae from control stained with rhodopsin 1 (Rh1) antibody. Flies were dissected after 0-6 hrs (day 0) and 12 hrs of bright light illumination (12h CL) post eclosion. Scale bar: 5 µm.

D. Quantification of RLVs from LS of retinae from control. The X-axis represents the time point and rearing condition. Y-axis shows the number of RLV's per ommatidium. n=10 ommatidia taken from three separate preps.

E. LS of retinae from control stained with Rh1 and Rab5; Rh1 and GFP (for *Rh1>GFP::Rab7*). Rearing condition is same as mentioned in (panel C). Scale bar: 5 µm.

F. Quantification of RLVs from LS of retinae from control. The X-axis represents the population of vesicles positive for mentioned protein. Y-axis shows the number of RLVs per ommatidium. n= 10 ommatidia taken from three separate preps.

G. Western blot from head extracts of control flies reared in various conditions as indicated on the top of the blot. The blot was probed with antibody to rhodopsin. Tubulin levels were used as a loading control.

H. Intensity response function of the light response from 4 day constant light (DAY 4 CL) and 4 day constant dark (DAY 4 CD) old control flies. The X-axis represents increasing light intensity in log units and Y-axis the peak response amplitude at each intensity normalized to the response at the maximum intensity. n=separate flies.

Data presented as mean +/-SEM

Figure 2: *dPLD* is required to support rhabdomere volume during illumination

A. TEM images showing single ommatidium from control and $dPLD^{3.1}$ .PRs of 0-12 hrs old flies post eclosion. Scale bar: 1 μm

B. Quantification of the rhabdomere volume of control and $dPLD^{3.1}$ .PRs reared in constant dark and constant light for 2 days post-eclosion. n=90 rhabdomeres taken from three separate flies.

C. Quantification of fold reduction in rhabdomere volume of control and $dPLD^{3.1}$ in light compared to dark. Genotypes are indicated on the X-axis and the Y-axis represents the percentage volume fraction (V_f) of the rhabdomere with respect to cell.

D. LS of retinae stained with rhodopsin 1 from $dPLD^{3.1}$. Rearing conditions are indicated. Scale bar: 5 μm.

E. Quantification of RLVs from LS of retinae from control and $dPLD^{3.1}$. n=10 ommatidia taken from three separate preps.

F. Quantification of RLVs from LS of retinae from control and $dPLD^{3.1}$ reared in 12h CL. The X-axis represents the population of vesicles positive for mentioned protein. Y-axis

shows the number of RLVs per ommatidium. n=10 ommatidia taken from three separate preps.

G. Western blot from head extracts of control (C) and *dPLD*$^{3.1}$ (P) of matched eye color. Rearing conditions as indicated on the top of the blot. The blot was probed with antibody to rhodopsin. Tubulin levels were used as a loading control.

H. Quantification of fold reduction of rhodopsin seen in *dPLD*$^{3.1}$ normalized to controls. The X-axis shows the genotype. Y-axis represents the fold reduction in rhodopsin. n=3.

I. Representative ERG responses of 0-12 hrs old flies to a single 2 s flash of green light. Genotypes are indicated. X-axis represents the time in seconds (s) and the Y-axis represents the amplitude of response in mV. The duration of light pulse is indicated.

J. Intensity response function of the light response of 0-12 hrs old flies. Responses from control and *dPLD*$^{3.1}$ flies with matched eye color are shown. The X-axis represents increasing light intensity in log units and Y-axis the peak response amplitude at each intensity normalized to the response at the maximum intensity. n= five separate flies. Data presented as mean +/-SEM

Figure 2 Supplement 1:

A. Schematic diagram representing the method used to generate the knockout of *Drosophila* phospholipase D (*dPLD*$^{3.1}$) using homologous recombination. The mutant allele generated with respect to the wild type locus is shown. The domains of dPLD (PX, PH, catalytic HKD1 and HKD2 and PIP_2 binding domains) are shown. The C-terminal domain is marked in red. A P^{w+} insertion (red box) that disrupts the HKD1 domain with

stop codons in all three frames on both strands (white boxes) is indicated as P[w+]. The last three amino acids at the C-terminus that have been mutated are shown as a black box. T5, T6 and T7 marks the primers designed in the HKD1 motif of dPLD.

B. PCR analysis for presence of HKD1 motif from crude genomic DNA extracts of WT (1) $dPLD^{3.1}$ (2) $dPLD^{3.1}$/Df(2R)ED1612 (3) and water control (4).One the left side of the gel picture primer pairs used are mentioned and on the right side the product lengths are indicated.

C. Total amounts of various phosphatidylcholine (PC) species extracted and measured from flies used for the transphosphatidylation assay experiment. The X-axis shows acyl chains species that were detected. Y-axis represents the mole percent of phosphatidylethanol species. Species measured from wild type and *dPLD*$^{3.1}$ with (10%) and without (0%) ethanol are shown.

D. The generation of phosphatidylethanol(P-EtOH) by dPLD (via the enzyme's transphosphatidylation activity) was measured. The X-axis shows acyl chains species that were detected. Y-axis represents the mole percent of phosphatidylethanol species. Species measured from wild type and *dPLD*$^{3.1}$ with (10%) and without (0%) ethanol are shown.

Figure 2 supplement 2:

A. Western blot from head extracts of control (C) and *dPLD*$^{3.1}$ (P) reared in various conditions as indicated on the top of the blot. The blot was probed with antibody to NORPA and TRP. Tubulin was used as loading control.

B. Confocal images of transverse section of retinae stained with an antibody to TRP in control and *dPLD*$^{3.1}$. Cross sections of the rhabdomere stained in red are shown. Scale bar 5 µm

Figure 2 supplement 3:

C. Representative ERG responses of 0-12 hrs old flies to a single 10 s flash of green light. Genotypes are indicated. X-axis represents the time in seconds (s) and the Y-axis represents the amplitude of response in mV. The duration of light pulse is indicated.

D. Quantification of the light response. Y-axis represents the ratio of final (A_f) and initial (A_i) amplitude of single trace during the stimulus in percentage. X-axis represents the genotypes. n = 3 separate flies

E. Representative ERG responses of 0-12 hrs old flies to a 1s flash of green light train - 5 pulses. Genotypes are indicated. X-axis represents the time in seconds (s) and the Y-axis represents the amplitude of response in mV. The duration of light pulse is indicated.

F. Quantification of the light response. Y-axis represents the ratio of final (A_f # 5 pulse) and initial (A_i # 1 pulse) amplitude during the stimulus in percentage. X-axis represents the genotypes. n = 3 separate flies

Data presented as mean +/-SEM

Figure 3: *dPLD* is essential to support rhabdomere structure during illumination

A. Representative optical neutralization (ON) images showing rhabdomere structure from control and $dPLD^{3.1}$ .The age and rearing conditions are mentioned on the top of the panels.

B. Quantification of rate of PR degeneration of control and $dPLD^{3.1}$ reared in bright light. The X-axis represents age of the flies and the Y-axis represents the number of intact rhabdomeres visualized in each ommatidium. n= 50 ommatidia taken from at least five separate flies.

C. TEM images showing a single ommatidium from control and $dPLD^{3.1}$ PRs reared in bright illumination for 6 days post eclosion. * indicates the collapsed rhabdomere and the arrow head indicate whorl like membranes accumulated in the cell body. Scale bar 1 µm.

D. Representative ON images showing ommatidia from $dPLD^{3.1}$*;Hs>dPLD* and $dPLD^{3.1}$*;Hs>*$dPLD^{K/R}$. The age and rearing conditions are indicated on the top of the image.

E. Quantification of rate of PR degeneration of control, $dPLD^{3.1}$, $dPLD^{3.1}$*;Hs>dPLD* and $dPLD^{3.1}$*;Hs>*$dPLD^{K/R}$ reared in bright light. n=50 ommatidia taken from at least five separate flies.

F. TEM images showing a single ommatidium from control, $dPLD^{3.1}$, $dPLD^{3.1}$*;Hs>dPLD* and $dPLD^{3.1}$*;Hs>*$dPLD^{K/R}$ PRs reared in light for 10 days post eclosion. Scale bar 1 µm. Data presented as mean +/-SEM

Figure 3 supplement 1:

A. Quantification of retinal degeneration in *dPLD$^{3.1}$*/+, *dPLD$^{1.1}$*/+, *dPLD$^{3.1}$*/ *dPLD$^{1.1}$*. The X-axis represents age of the flies and the Y-axis represents the number of rhabdomere visualized in each ommatidium. Error bars represents mean +/- S.E.M from 50 ommatidia taken from at least five separate flies.

B. Quantification of retinal degeneration in *control*, *dPLD$^{3.1}$*, *dPLD$^{3.1}$*/ *dPLD$^{1.1}$*. The X-axis represents age of the flies and the Y-axis represents the number of rhabdomere visualized in each ommatidium. Error bars represents mean +/- S.E.M from 50 ommatidia taken from at least five separate flies.

C. Quantification of retinal degeneration in *Df(2R)ED1612*/+, *dPLD$^{3.1}$*, *dPLD$^{3.1}$*/*Df(2R)ED1612*. The X-axis represents age of the flies and the Y-axis represents the number of rhabdomere visualized in each ommatidium. Error bars represents mean +/- S.E.M from 50 ommatidia taken from at least five separate flies.

Figure 4: Phosphatidic acid levels and retinal degeneration in *dPLD$^{3.1}$*

A. Total PC level in retinae of control and *dPLD$^{3.1}$*. The X-axis represents the genotypes and the Y-axis shows the level of PC as pmole/µmole of total lipid phosphate present in the sample. n=3.

B. Total PA level in retinae of control and *dPLD$^{3.1}$*. The X-axis represents the genotypes and the Y-axis shows the level of PA as pmole/µmole of total lipid phosphate present in the sample. n=3

C. Molecular species of PA in retinae of control and *dPLD$^{3.1}$*. X-axis shows the acyl chain composition of each species predicted from its monoisotopic peaks and corresponding

elemental composition constraints. Y-axis shows the abundance of each species as pmole/µmole of total lipid phosphate present in the sample. n=3.

D. PA levels in heads extracts of control, *dPLD*$^{3.1}$, *dPLD*$^{3.1}$*;Hs>dPLD* and *dPLD*$^{3.1}$*;Hs>dPLD*$^{K/R}$ .n=3

E. Quantification of retinal degeneration seen in control, *laza*^{22}, *dPLD*$^{3.1}$ and *dPLD*$^{3.1}$*;laza*^{22}. n= 50 ommatidia taken from at least five separate flies.

F. PA levels in heads extracts of control, *laza*^{22}, *dPLD*$^{3.1}$ and *dPLD*$^{3.1}$*;laza*^{22} n=3.

G. PA levels from retinal extracts of *Gq*^{1} and *Gq*^{1}*,dPLD*$^{3.1}$. Flies were reared in complete darkness and post ecclosion one set of flies were shifted to bright illumination for 12 hrs while the others kept in darkness for 12 hrs. n=3.

H. LS of retinae stained with Rh1 from *Rh1>dPLD* and *Rh1>dPLD*$^{K/R}$. Rearing conditions are indicated at the top of panels. Scale bar:5 µm.

I. Quantification of RLVs from LS of retinae from control, *Rh1>dPLD* and *Rh1>dPLD*$^{K/R}$. n=10 ommatidia taken from three separate preps.

Data presented as mean +/-SEM

Figure 4 supplement 1:

A. Quantification of retinal degeneration in control, *Rh1>rdgA, dPLD*$^{3.1}$*, dPLD*$^{3.1}$*;Rh1>rdgA*. The X-axis represents age of the flies and the Y-axis represents the number of rhabdomere visualized in each ommatidium. Error bars represents mean +/- S.E.M from 50 ommatidia taken from at least five separate flies.

B. PA levels in heads extracts. Genotypes indicated on X-axis. Y-axis shows the total PA as pmole/µmole of total lipid phosphate present in the sample. Error bars indicate the mean +/- SEM from three separate analyses.

Figure 5: dPLD activity supports the removal of RLVs from the cell body during illumination

A. Quantification of RLVs from LS of retinae from control and *shi^{ts1}*. n= 10 ommatidia taken from three separate preps.

B. Quantification of RLVs from LS of retinae from *shi^{ts1}* and *shi^{ts1};dPLD$^{3.1}$*. n= 10 ommatidia taken from three separate preps.

C. LS of retinae stained with Rh1 from *norpA^{P24}* and *norpA^{P24};Rh1>dPLD*. Rearing condition is indicated at the top of each panel. Scale bar: 5 µm.

D. Quantification of RLVs from LS of retinae from control, *norpA^{P24}* and *norpA^{P24};Rh1>dPLD*. n=10 ommatidia taken from three separate preps.

E. TEM images showing single ommatidium from control, *norpA^{P24}*, *Rh1>dPLD* and *norpA^{P24};Rh1>dPLD* PRs of flies. * indicates the degenerated rhabdomere. Rearing condition is indicated on the top of the image. Scale bar: 1 µm.

F. Quantification of retinal degeneration in control, *norpA^{P24}* and *norpA^{P24};Rh1>dPLD* done using TEM images. The Y-axis represents the number of rhabdomeres visualized in each ommatidium. n=50 ommatidia taken from at least two separate flies.

G. Quantification of RLVs from LS of retinae from *Rh1>dPLD* in dark vs light(12h CL). The X-axis represents the population of vesicles positive for mentioned protein. Y-axis shows the number of RLV's per ommatidium. n=10 ommatidia taken from three separate preps.

Data presented as mean +/-SEM

Figure 6: dPLD regulates clearance of RLVs via retromer function

A. LS of retinae stained with Rh1 from *Rh1>Dicer,vps35^{RNAi}*. Rearing conditions are indicated at the top of panels. Scale bar:5 μm

B. Quantification of RLVs from LS of retinae *control* and *Rh1>Dicer,vps35^{RNAi} .* n=10 ommatidia taken from three separate preps.

C. Quantification of retinal degeneration in *control*, *dPLD$^{3.1}$, Rh1>vps35* and *dPLD$^{3.1}$;Rh1>vps35*. n=50 ommatidia taken from at least five separate flies.

D. Quantification of RLVs from LS of retinae from *control*, *dPLD$^{3.1}$, Rh1>vps35* and *dPLD$^{3.1}$;Rh1>vps35* . n=10 ommatidia taken from three separate preps.

E. Longitudinal section of retinae stained with Rh1 *Rh1>dPLD; Dicer,vps35^{RNAi}*. Rearing condition is indicated at the top of each panel. Scale bar: 5 μm.

F. Quantification of RLVs from longitudinal section of retinae from *control*, *Rh1>Dicer,vps35^{RNAi}, Rh1>dPLD* and *Rh1>dPLD; Dicer,vps35^{RNAi}*. n=10 ommatidia taken from three separate preps.

Data presented as mean +/-SEM

Figure 7: Arf1 activity and retinal degeneration in *dPLD$^{3.1}$*

A. Quantification of RLVs from longitudinal section of retinae from control and *Rh1>garz*. n=10 ommatidia taken from three separate preps.

B. TEM images showing single ommatidium from *Rh1>garz* and *dPLD$^{3.1}$;Rh1>garz* PRs of flies. Rearing condition is indicated on the top of the image. Scale bar: 1 μm.

C. Quantification of retinal degeneration in control, *dPLD$^{3.1}$, Rh1>garz* and *dPLD$^{3.1}$;Rh1>garz*. n=50 ommatidia taken from at least five separate flies.

D. TEM images showing single ommatidium from *Rh1>garz*^{RNAi} PRs of flies. Rearing condition is indicated on the image. Scale bar:1 μm.

E. Quantification showing the retinal degeneration in control, *dPLD*$^{3.1}$ and *Rh1>garz*^{RNAi}. n= 50 ommatidia taken from at least five separate flies.

G. Quantification of RLVs from longitudinal section of retinae from control, *dPLD*$^{3.1}$, *dPLD*$^{3.1}$*;Rh1>garz*. n=10 ommatidia taken from three separate preps.

Data presented as mean +/-SEM

Figure 8: *dPLD* and *garz* are required for RLV clearance during illumination

A. Quantification of RLVs from longitudinal section of retinae from control, *Rh1>dPLD*, *Rh1>dPLD ;Dicer,Rh1>garz*^{RNAi}. n= 10 ommatidia taken from three separate preps.

B. Quantification of RLVs from longitudinal section of retinae from control, *Rh1>garz, Rh1>Dicer,vps35*^{RNAi} and *Rh1>garz;Dicer,vps35*^{RNAi}. n=10 ommatidia taken from three separate preps.

C. TEM images showing single ommatidium from control and *dPLD*$^{3.1}$,Rh1>*Arf1*^{CA} and *dPLD*$^{3.1}$;Rh1>*Arf1*^{CA} PRs of day 0-old flies post eclosion. Scale bar: 1 μm

D. A model of the light activated turnover of rhabdomere membranes in *Drosophila* photoreceptors. The cross section of a PR is shown. The area indicated by the red box is enlarged to the left. PC-phosphatidylcholine, PA-phosphatidic acid, dARF1-GTP-GTP bound active ARF1, dARF1-GDP-GDP bound inactive Arf1, brown star indicates retromer, blue RLVs indicate endocytic compartment while orange RLVs indicate recycling compartment.

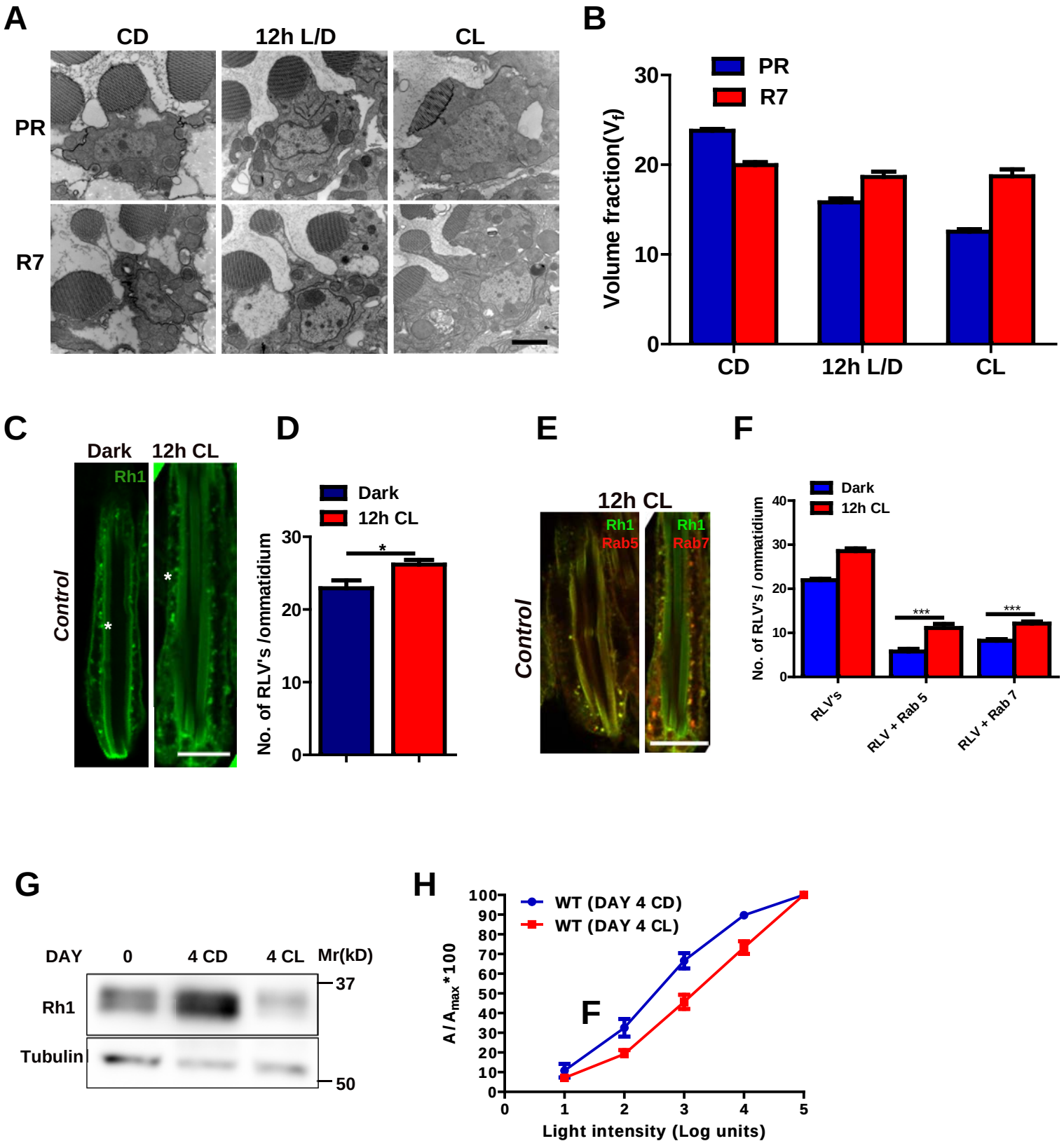
A
CD
12h L/D
CL
PR
R7
B
PR
R7
Volume fraction(Vf)
30
20
10
0
CD
12h L/D
CL
C
Dark
12h CL
Rh1
Control
D
Dark
12h CL
No. of RLV's /ommatidium
30
20
10
0
*
E
12h CL
Rh1
Rab5
Rh1
Rab7
Control
F
Dark
12h CL
No. of RLV's / ommatidium
40
30
20
10
0
***
***
RLV's
RLV + Rab 5
RLV + Rab 7
G
DAY
0
4 CD
4 CL
Mr(kD)
Rh1
Tubulin
37
50
H
WT (DAY 4 CD)
WT (DAY 4 CL)
A / Amax *100
100
90
80
70
60
50
40
30
20
10
0
F
0
1
2
3
4
5
Light intensity (Log units)

Figure 1

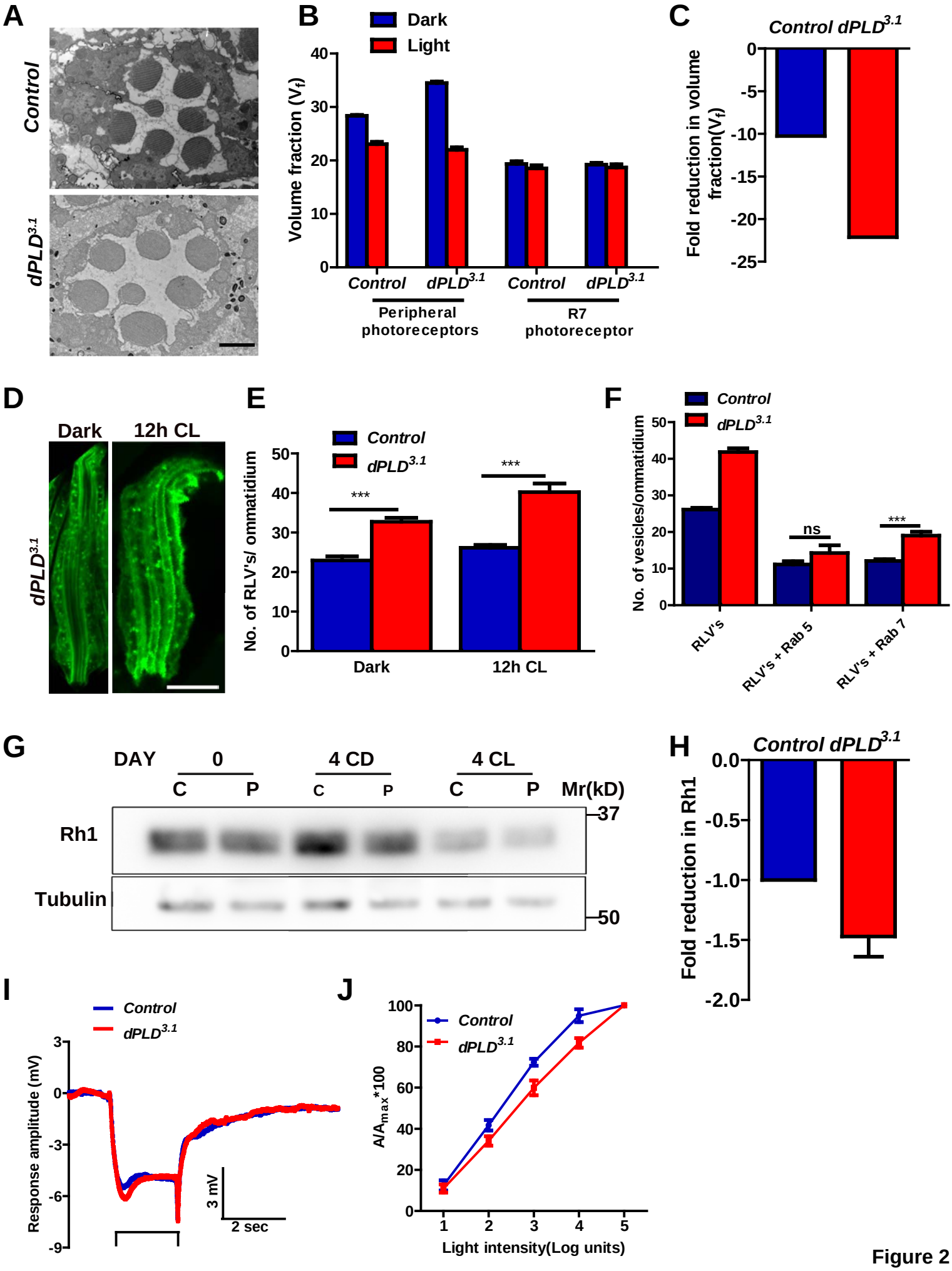
A
Control
dPLD3.1
B
Dark
Light
Volume fraction (Vf)
40
30
20
10
0
Control
dPLD3.1
Control
dPLD3.1
Peripheral photoreceptors
R7 photoreceptor
C
Control dPLD3.1
Fold reduction in volume fraction(Vf)
0
-5
-10
-15
-20
-25
D
Dark
12h CL
dPLD3.1
E
Control
dPLD3.1
No. of RLV's/ ommatidium
50
40
30
20
10
0
***
***
Dark
12h CL
F
Control
dPLD3.1
No. of vesicles/ommatidium
50
40
30
20
10
0
ns
***
RLV's
RLV's + Rab 5
RLV's + Rab 7
G
DAY
0
4 CD
4 CL
C
P
C
P
C
P
Mr(kD)
Rh1
37
Tubulin
50
H
Control dPLD3.1
Fold reduction in Rh1
0.0
-0.5
-1.0
-1.5
-2.0
I
Control
dPLD3.1
Response amplitude (mV)
3
0
-3
-6
-9
3 mV
2 sec
J
Control
dPLD3.1
A/Amax*100
100
80
60
40
20
0
1
2
3
4
5
Light intensity(Log units)

Figure 2

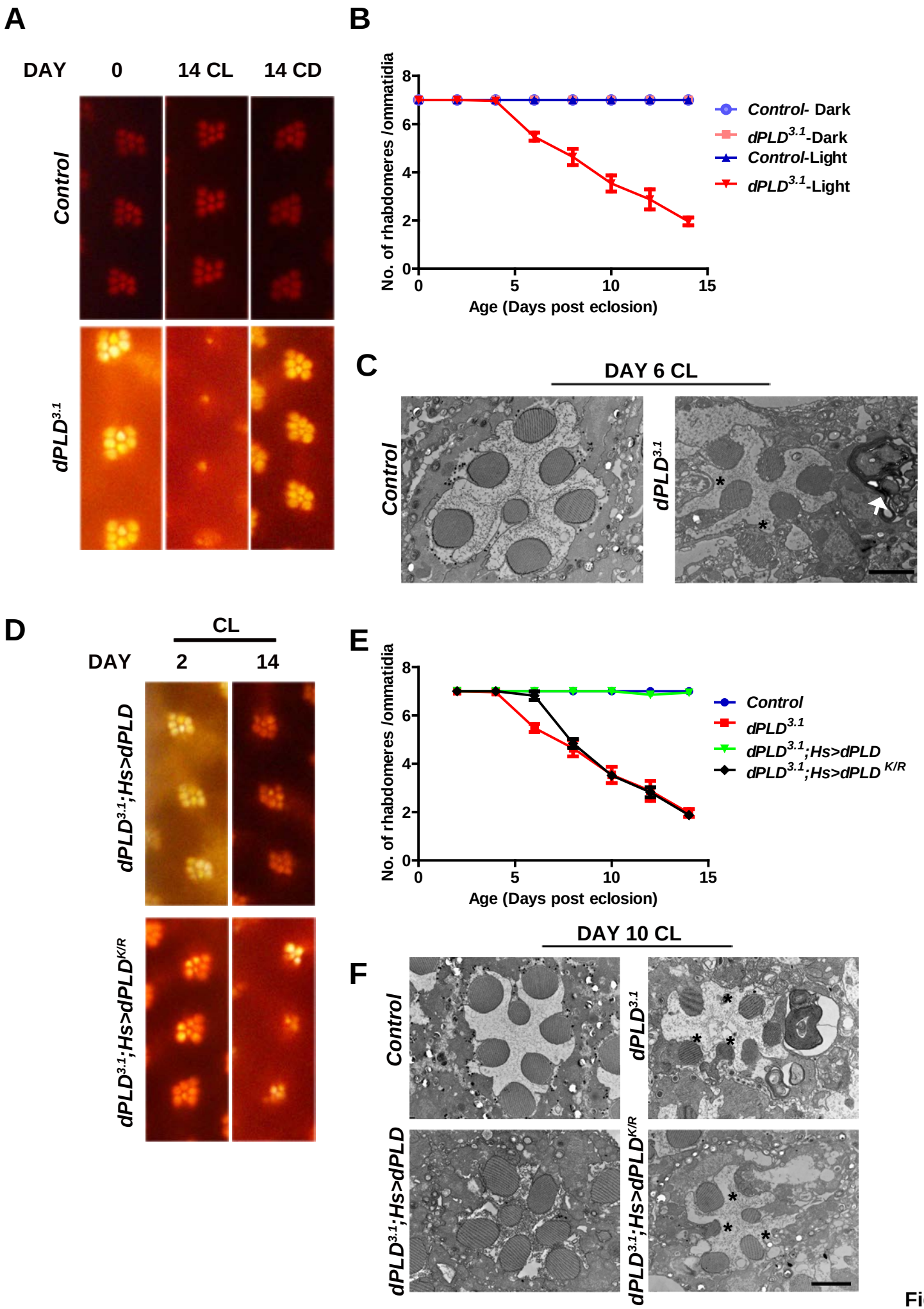
A
DAY
0
14 CL
14 CD
Control
dPLD3.1
B
No. of rhabdomeres /ommatidia
Age (Days post eclosion)
Control- Dark
dPLD3.1-Dark
Control-Light
dPLD3.1-Light
C
DAY 6 CL
Control
dPLD3.1
D
CL
DAY
2
14
dPLD3.1;Hs>dPLD
dPLD3.1;Hs>dPLDK/R
E
No. of rhabdomeres /ommatidia
Age (Days post eclosion)
Control
dPLD3.1
dPLD3.1;Hs>dPLD
dPLD3.1;Hs>dPLD K/R
F
DAY 10 CL
Control
dPLD3.1
dPLD3.1;Hs>dPLD
dPLD3.1;Hs>dPLDK/R

Figure 3

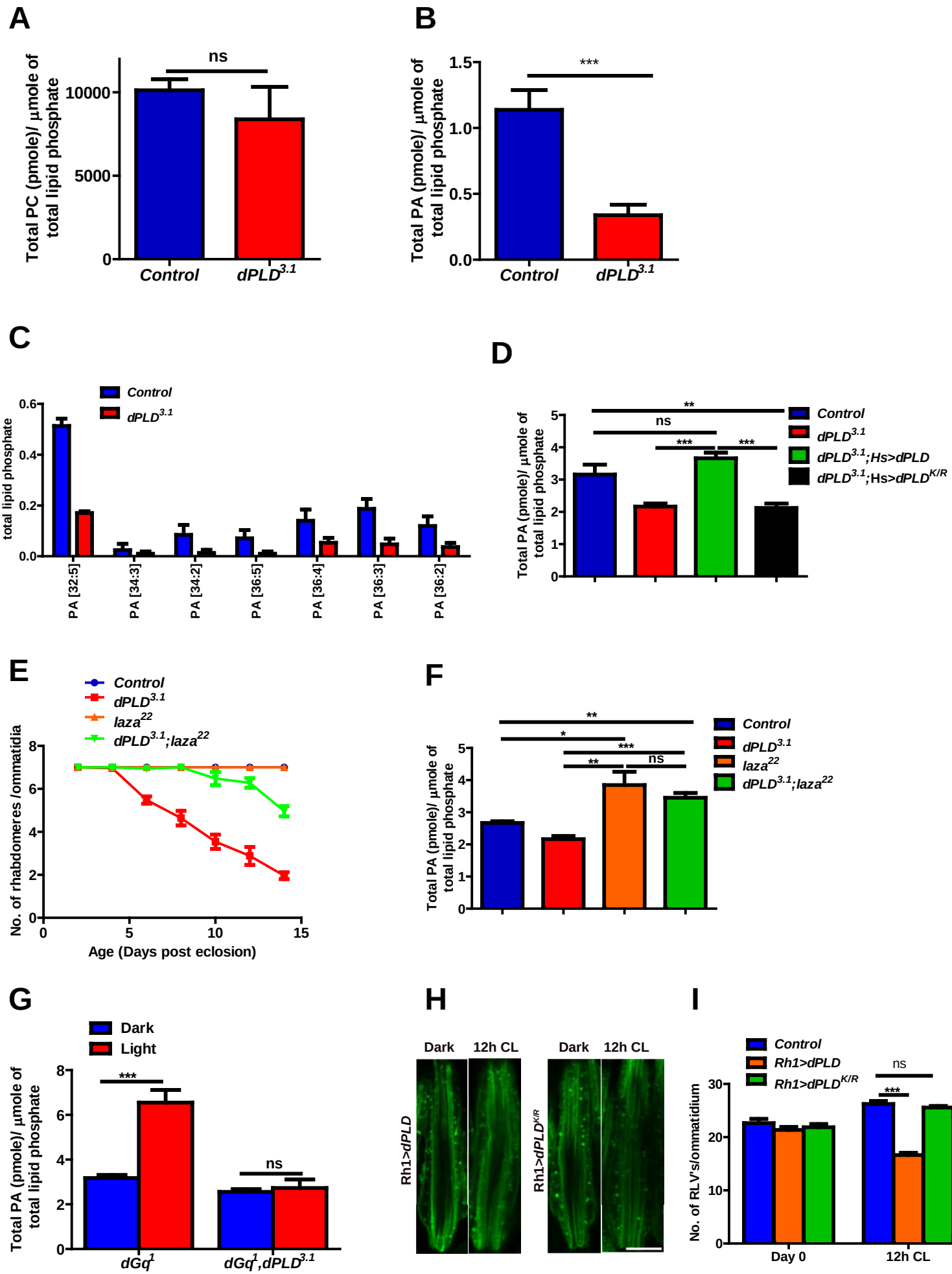
A
Total PC (pmole)/ µmole of total lipid phosphate
10000
5000
0
ns
Control
dPLD3.1
B
Total PA (pmole)/ µmole of total lipid phosphate
1.5
1.0
0.5
0.0
***
Control
dPLD3.1
C
Control
dPLD3.1
pmole/ µmole of total lipid phosphate
0.6
0.4
0.2
0.0
PA [32:5]
PA [34:3]
PA [34:2]
PA [36:5]
PA [36:4]
PA [36:3]
PA [36:2]
D
Total PA (pmole)/ µmole of total lipid phosphate
5
4
3
2
1
0
**
ns
***
***
Control
dPLD3.1
dPLD3.1;Hs>dPLD
dPLD3.1;Hs>dPLDK/R
E
Control
dPLD3.1
laza22
dPLD3.1;laza22
No. of rhabdomeres /ommatidia
8
6
4
2
0
0
5
10
15
Age (Days post eclosion)
F
Total PA (pmole)/ µmole of total lipid phosphate
5
4
3
2
1
0
**
*
***
**
ns
Control
dPLD3.1
laza22
dPLD3.1;laza22
G
Dark
Light
Total PA (pmole)/ µmole of total lipid phosphate
8
6
4
2
0
***
ns
dGq1
dGq1,dPLD3.1
H
Dark
12h CL
Dark
12h CL
Rh1>dPLD
Rh1>dPLDK/R
I
Control
Rh1>dPLD
Rh1>dPLDK/R
No. of RLV's/ommatidium
30
20
10
0
ns
***
Day 0
12h CL

Figure 4

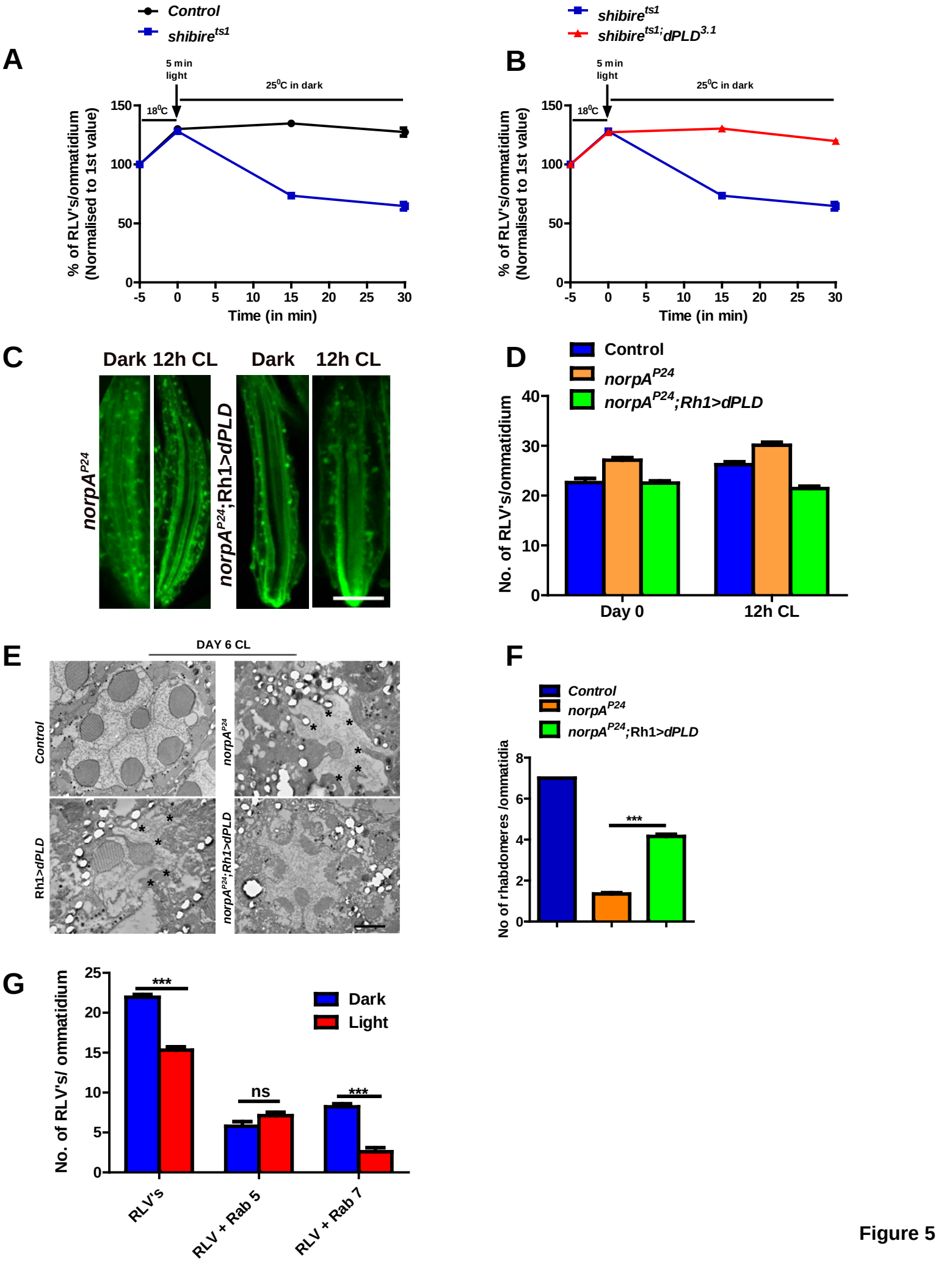
A
Control
shibire^ts1
5 min light
25°C in dark
18°C
% of RLV's/ommatidium (Normalised to 1st value)
Time (in min)
B
shibire^ts1
shibire^ts1;dPLD3.1
C
Dark 12h CL
Dark 12h CL
norpA^P24
norpA^P24;Rh1>dPLD
D
Control
norpA^P24
norpA^P24;Rh1>dPLD
No. of RLV's/ommatidium
Day 0
12h CL
E
DAY 6 CL
Control
norpA^P24
Rh1>dPLD
norpA^P24;Rh1>dPLD
F
Control
norpA^P24
norpA^P24;Rh1>dPLD
No of rhabdomeres /ommatidia
***
G
No. of RLV's/ ommatidium
Dark
Light
***
ns
***
RLV's
RLV + Rab 5
RLV + Rab 7

Figure 5

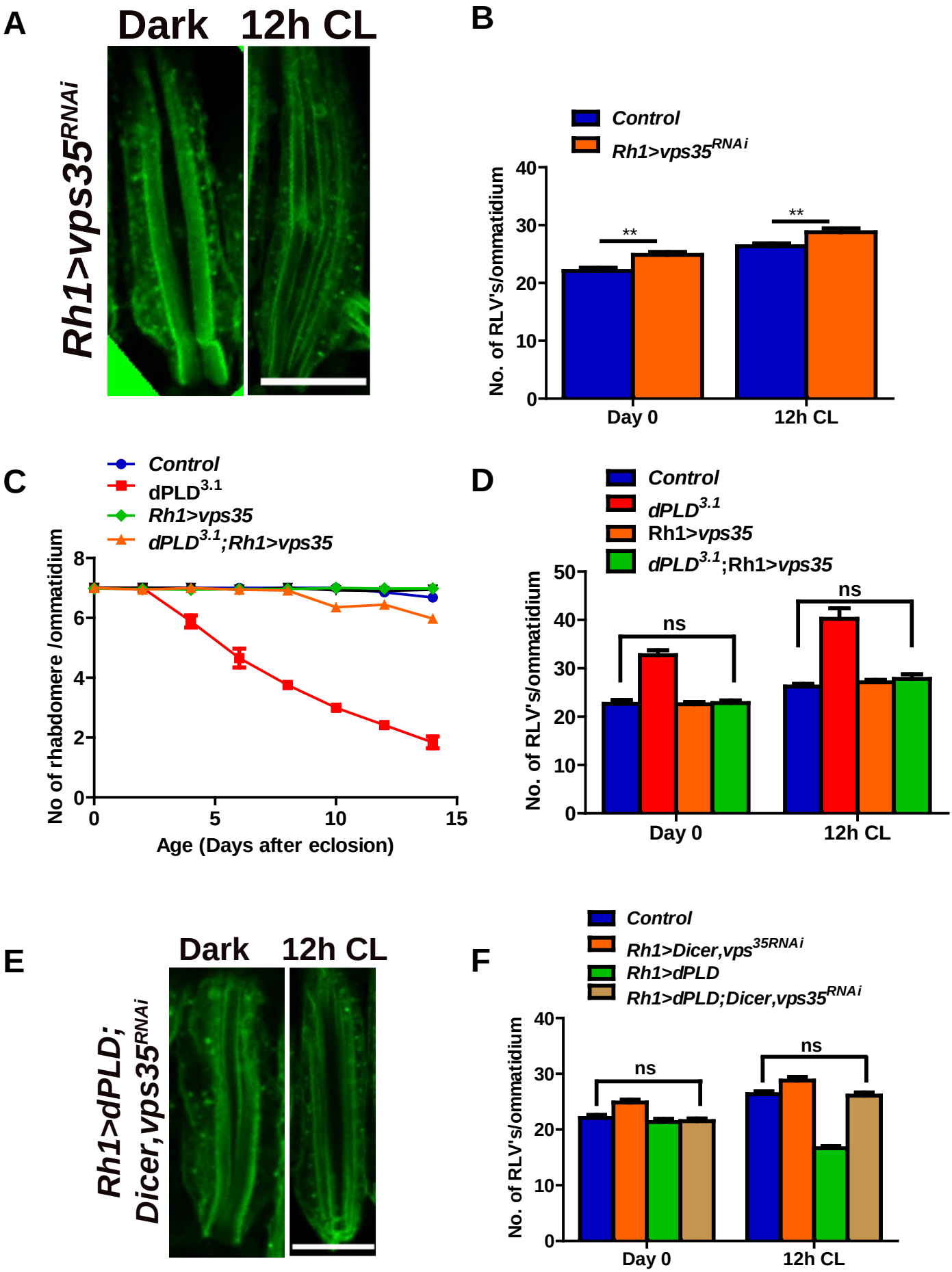
A
Dark
12h CL
Rh1>vps35RNAi
B
Control
Rh1>vps35RNAi
No. of RLV's/ommatidium
40
30
20
10
0
**
**
Day 0
12h CL
C
Control
dPLD3.1
Rh1>vps35
dPLD3.1;Rh1>vps35
No of rhabdomere /ommatidium
8
6
4
2
0
0
5
10
15
Age (Days after eclosion)
D
Control
dPLD3.1
Rh1>vps35
dPLD3.1;Rh1>vps35
No. of RLV's/ommatidium
50
40
30
20
10
0
ns
ns
Day 0
12h CL
E
Dark
12h CL
Rh1>dPLD;
Dicer,vps35RNAi
F
Control
Rh1>Dicer,vps35RNAi
Rh1>dPLD
Rh1>dPLD;Dicer,vps35RNAi
No. of RLV's/ommatidium
40
30
20
10
0
ns
ns
Day 0
12h CL

Figure 6

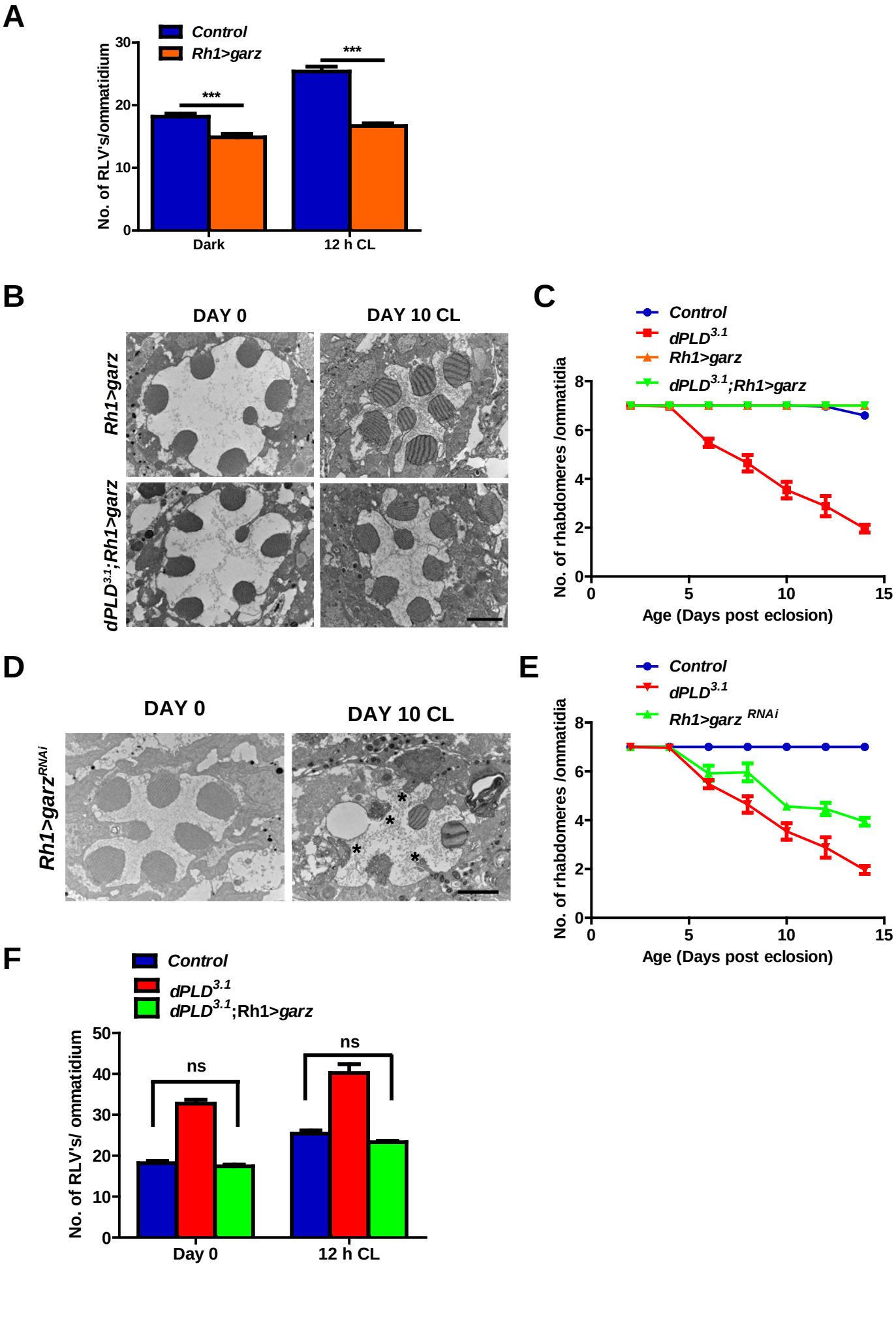
A
Control
Rh1>garz
No. of RLV's/ommatidium
30
20
10
0
***
***
Dark
12 h CL
B
DAY 0
DAY 10 CL
Rh1>garz
dPLD3.1;Rh1>garz
C
Control
dPLD3.1
Rh1>garz
dPLD3.1;Rh1>garz
No. of rhabdomeres /ommatidia
8
6
4
2
0
0
5
10
15
Age (Days post eclosion)
D
DAY 0
DAY 10 CL
Rh1>garzRNAi
E
Control
dPLD3.1
Rh1>garz RNAi
No. of rhabdomeres /ommatidia
8
6
4
2
0
0
5
10
15
Age (Days post eclosion)
F
Control
dPLD3.1
dPLD3.1;Rh1>garz
No. of RLV's/ ommatidium
50
40
30
20
10
0
ns
ns
Day 0
12 h CL

Figure 7

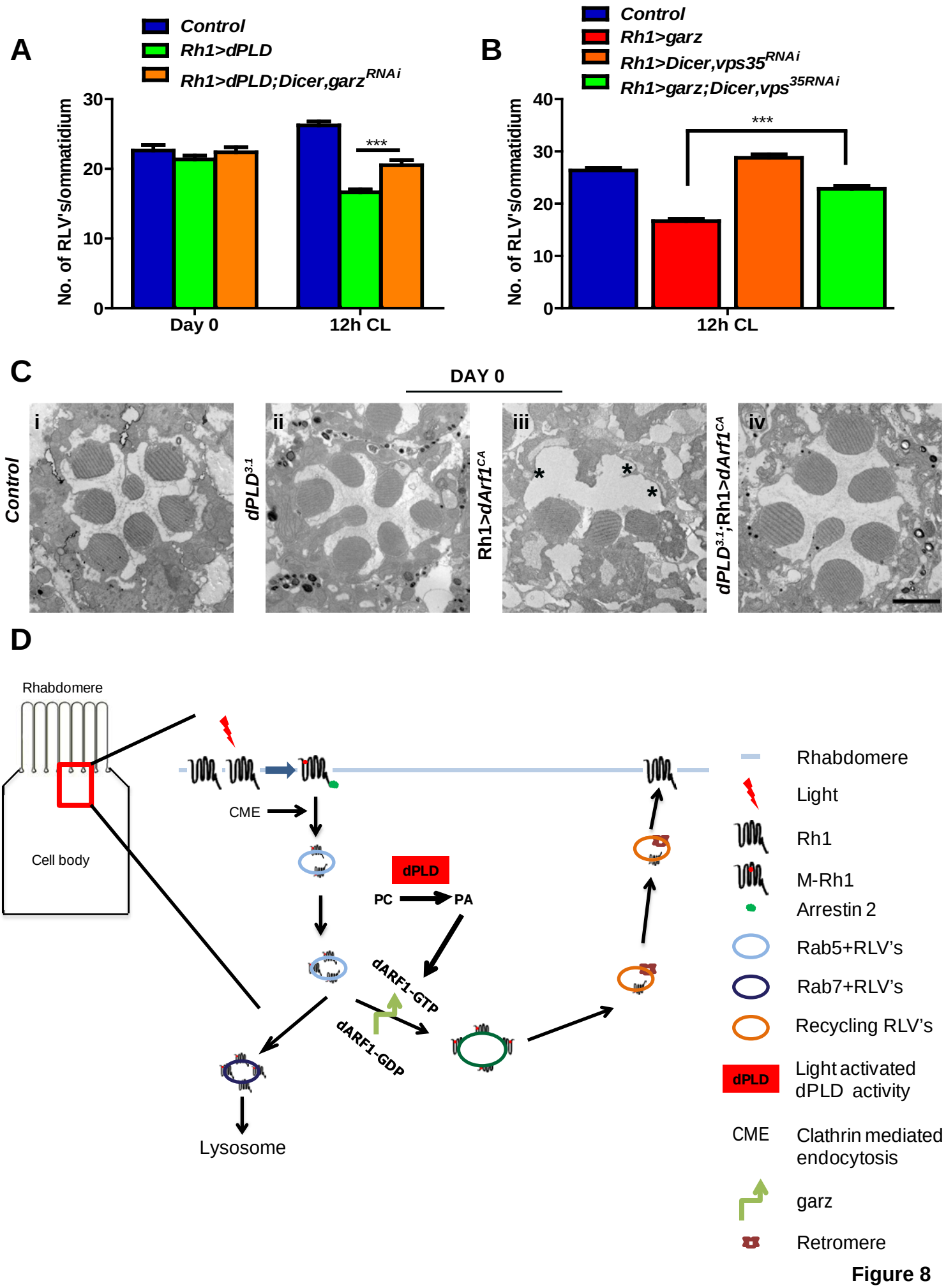
A
Control
Rh1>dPLD
Rh1>dPLD;Dicer,garz RNAi
No. of RLV's/ommatidium
30
20
10
0
***
Day 0
12h CL
B
Control
Rh1>garz
Rh1>Dicer,vps35 RNAi
Rh1>garz;Dicer,vps 35RNAi
No. of RLV's/ommatidium
40
30
20
10
0
***
12h CL
C
DAY 0
Control
i
dPLD3.1
ii
Rh1>dArf1CA
iii
dPLD3.1;Rh1>dArf1CA
iv
D
Rhabdomere
CME
Cell body
dPLD
PC
PA
dARF1-GTP
dARF1-GDP
Lysosome
Rhabdomere
Light
Rh1
M-Rh1
Arrestin 2
Rab5+RLV's
Rab7+RLV's
Recycling RLV's
dPLD
Light activated dPLD activity
CME
Clathrin mediated endocytosis
garz
Retromere

Figure 8

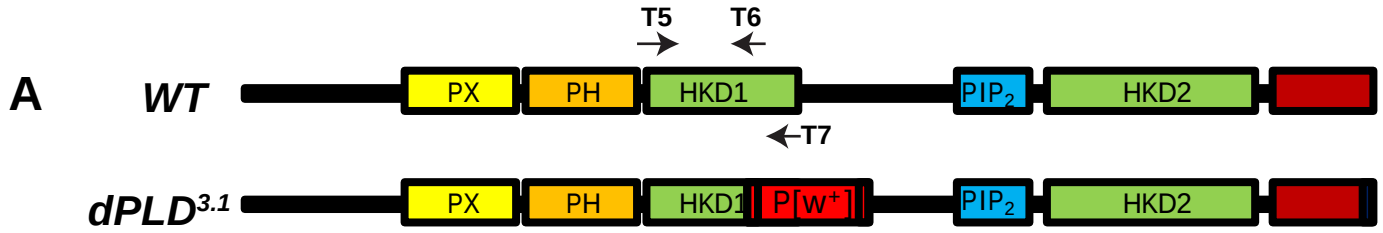
A
WT
T5
T6
PX
PH
HKD1
PIP2
HKD2
T7
dPLD3.1
P[w+]

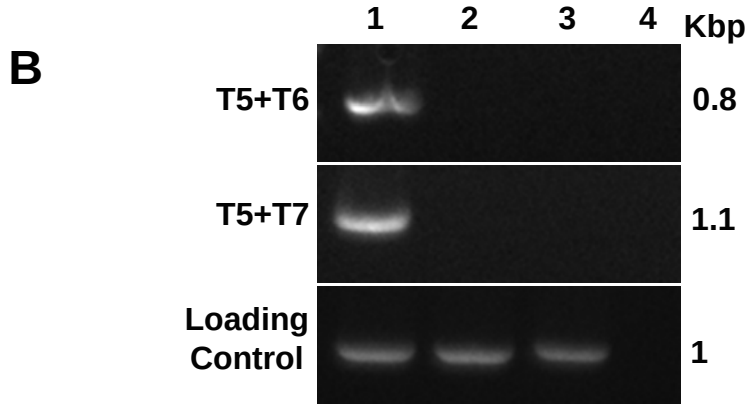
B
1
2
3
4
Kbp
T5+T6
0.8
T5+T7
1.1
Loading Control
1

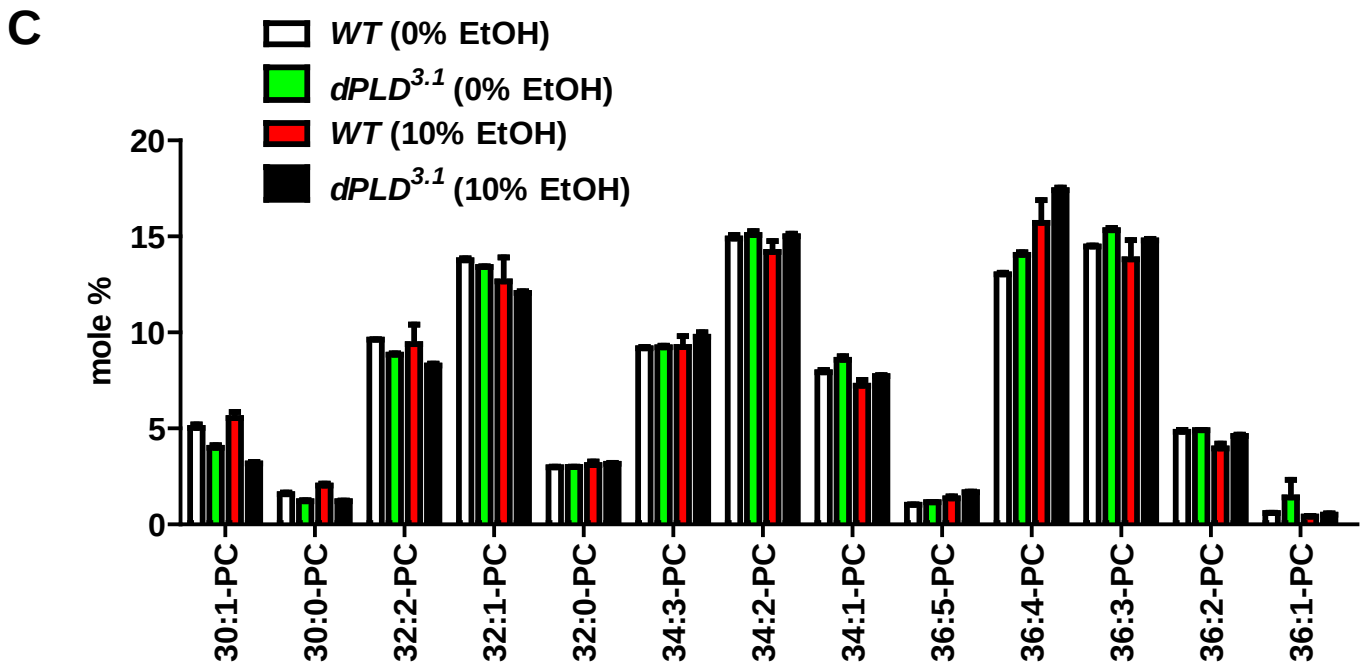
C
WT (0% EtOH)
dPLD3.1 (0% EtOH)
WT (10% EtOH)
dPLD3.1 (10% EtOH)
mole %
20
15
10
5
0
30:1-PC
30:0-PC
32:2-PC
32:1-PC
32:0-PC
34:3-PC
34:2-PC
34:1-PC
36:5-PC
36:4-PC
36:3-PC
36:2-PC
36:1-PC

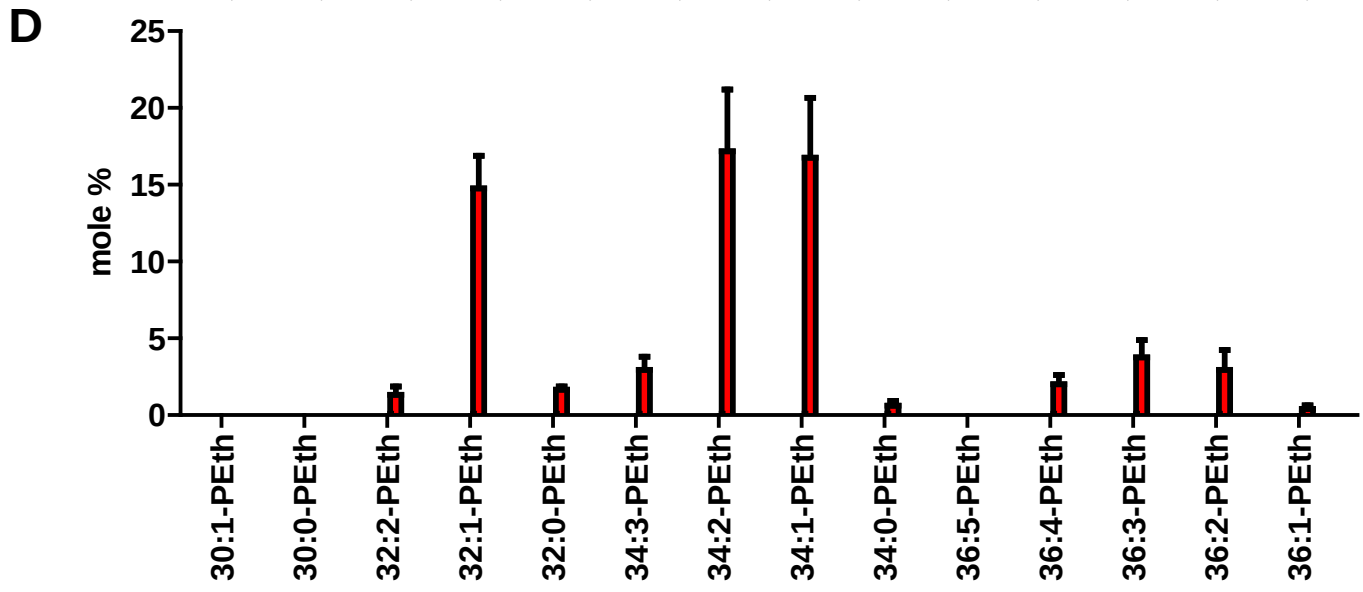
D
mole %
25
20
15
10
5
0
30:1-PEth
30:0-PEth
32:2-PEth
32:1-PEth
32:0-PEth
34:3-PEth
34:2-PEth
34:1-PEth
34:0-PEth
36:5-PEth
36:4-PEth
36:3-PEth
36:2-PEth
36:1-PEth

Figure 2 S1

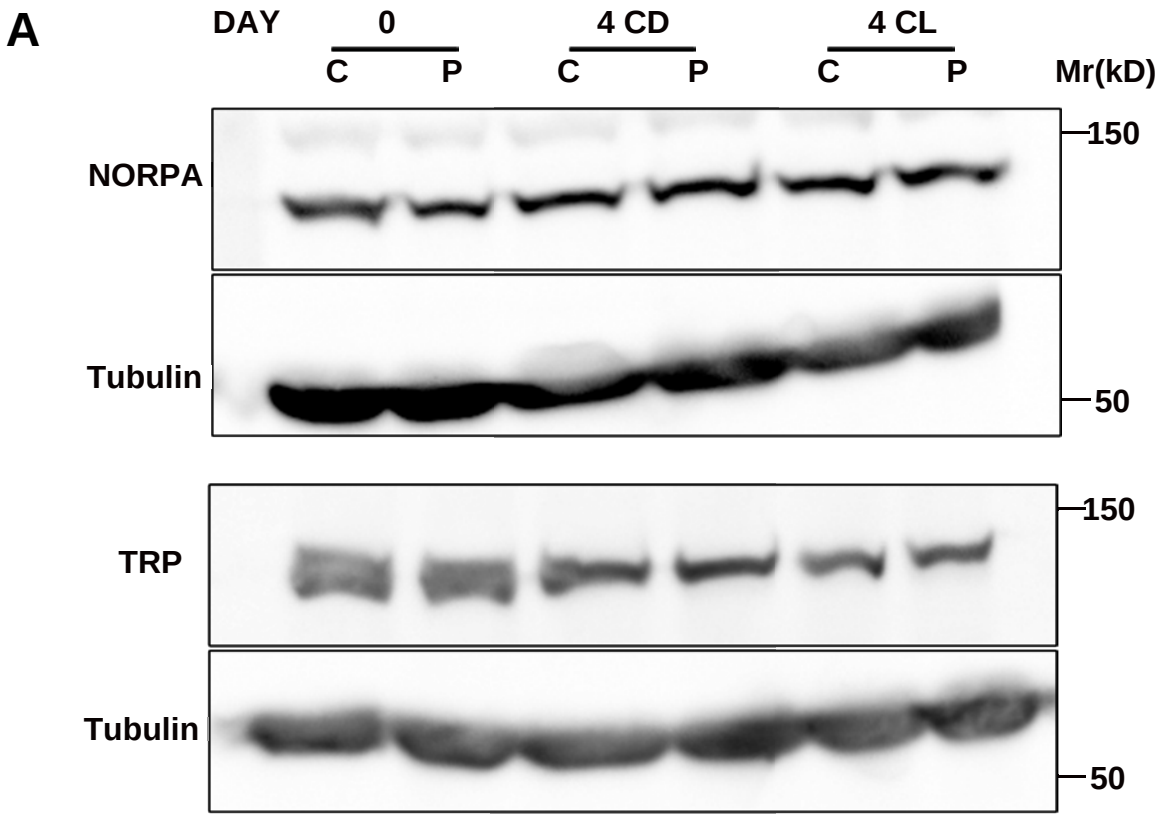
A
DAY
0
4 CD
4 CL
C
P
C
P
C
P
Mr(kD)
NORPA
150
Tubulin
50
TRP
150
Tubulin
50

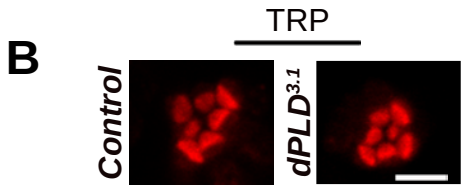
B
TRP
Control
dPLD3.1

Figure 2 S2

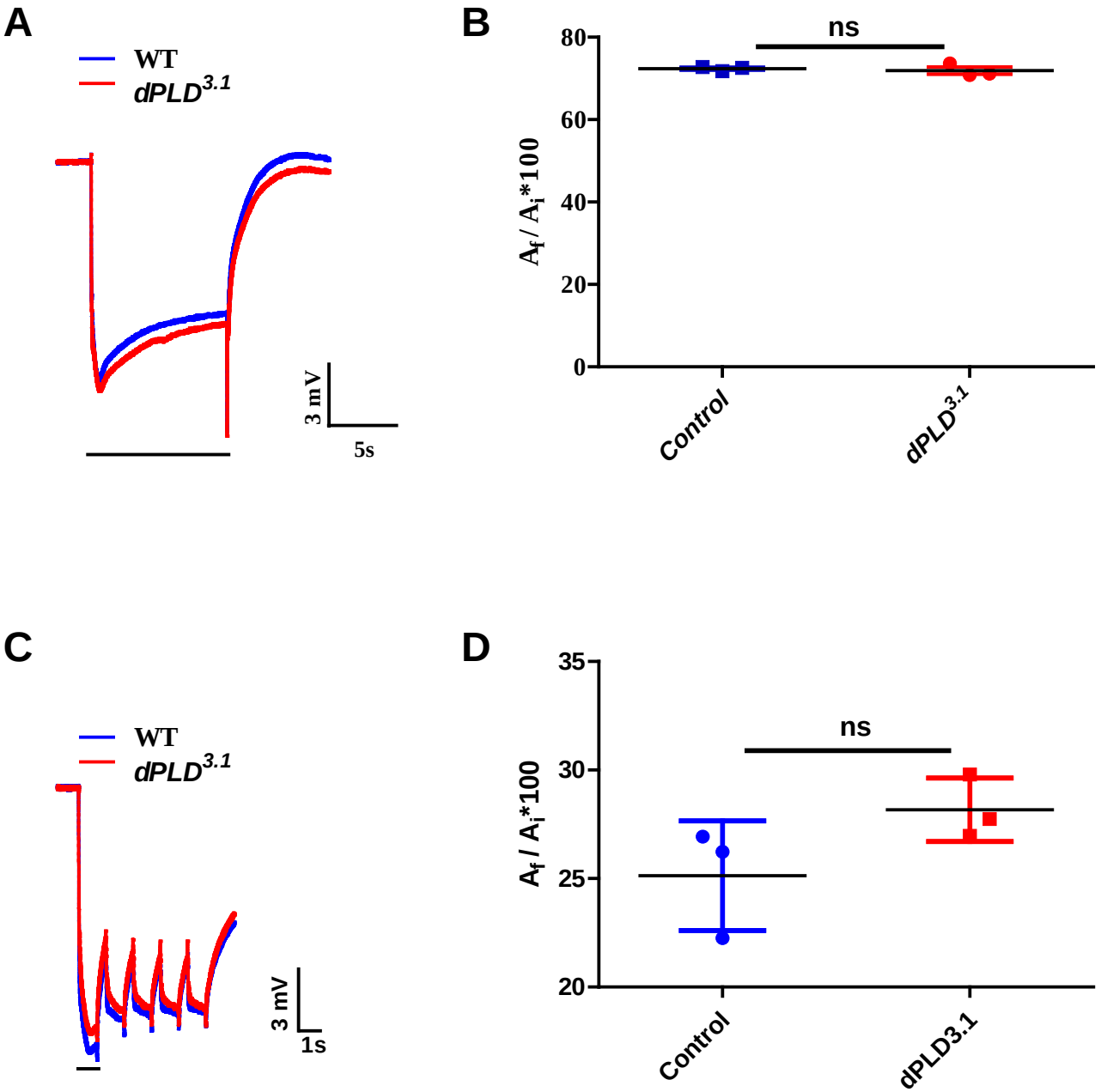
A
WT
dPLD3.1
3 mV
5s
B
ns
80
60
40
20
0
Af / Ai*100
Control
dPLD3.1
C
WT
dPLD3.1
3 mV
1s
D
ns
35
30
25
20
Af / Ai*100
Control
dPLD3.1

Figure 2 S3

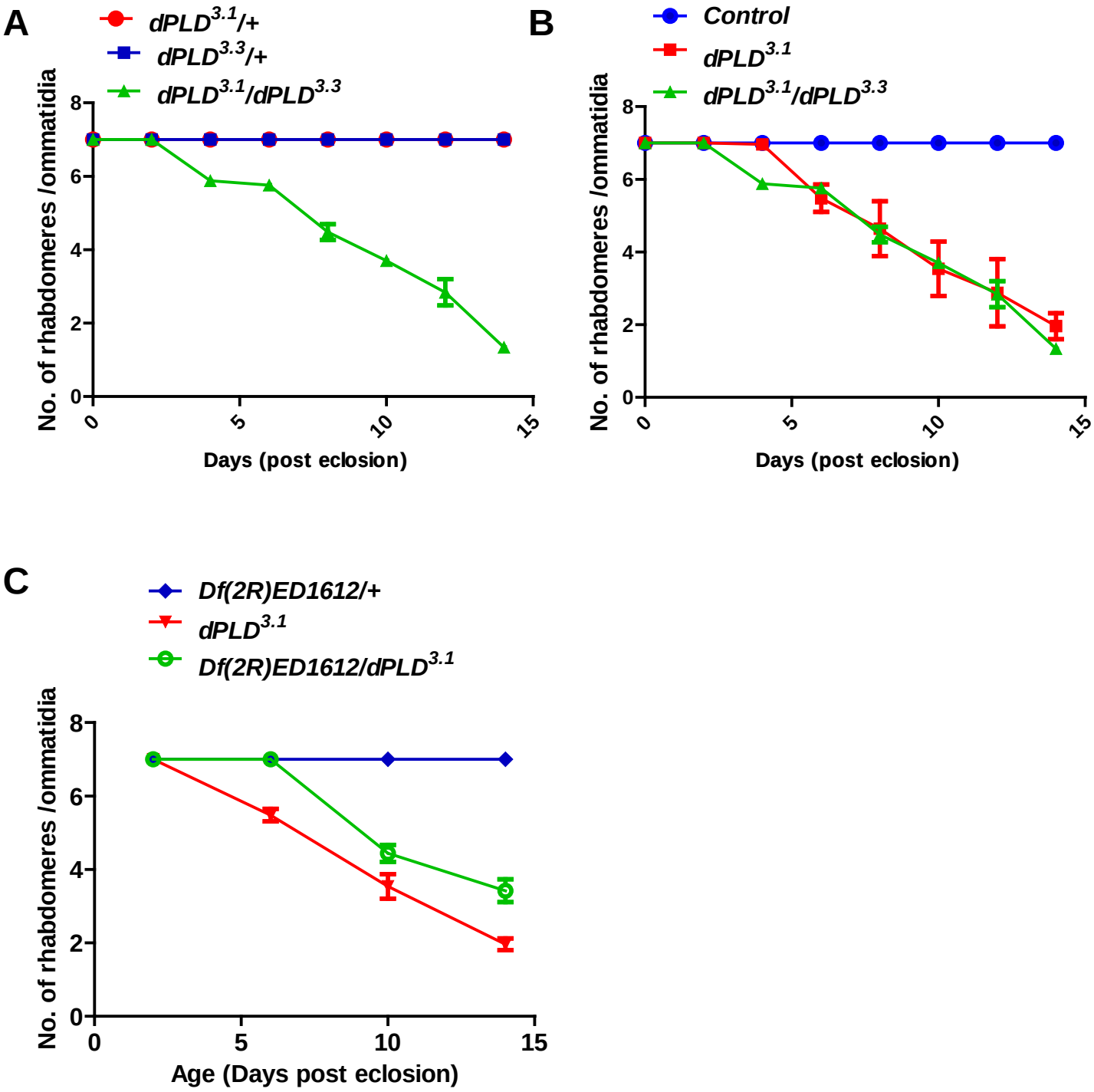
A
dPLD3.1/+
dPLD3.3/+
dPLD3.1/dPLD3.3
No. of rhabdomeres /ommatidia
Days (post eclosion)
B
Control
dPLD3.1
dPLD3.1/dPLD3.3
No. of rhabdomeres /ommatidia
Days (post eclosion)
C
Df(2R)ED1612/+
dPLD3.1
Df(2R)ED1612/dPLD3.1
No. of rhabdomeres /ommatidia
Age (Days post eclosion)

Figure 3 S1

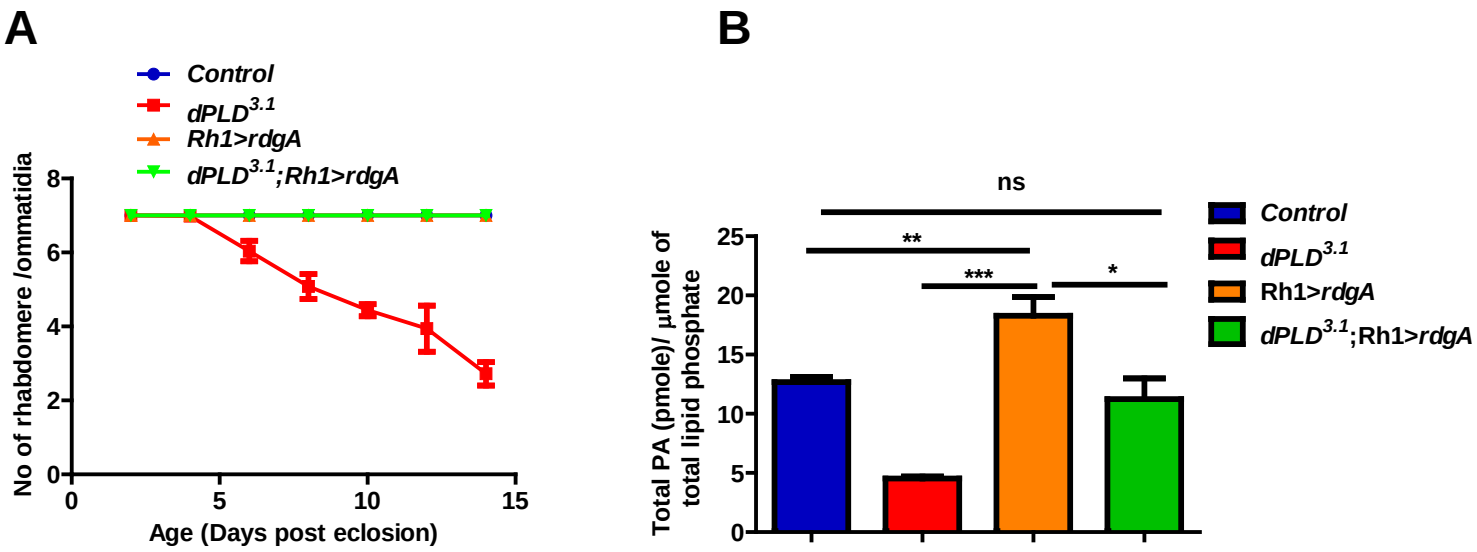
A
Control
dPLD3.1
Rh1>rdgA
dPLD3.1;Rh1>rdgA
No of rhabdomere /ommatidia
0
2
4
6
8
0
5
10
15
Age (Days post eclosion)
B
ns
**
***
*
Total PA (pmole)/ µmole of total lipid phosphate
0
5
10
15
20
25
Control
dPLD3.1
Rh1>rdgA
dPLD3.1;Rh1>rdgA

Figure 4 S1